

Deterministic remote preparation of multi-qubit equatorial states through dissipative channels

Liu-Yong Cheng(程留永), Shi-Feng Zhang(张世凤), Zuan Meng(孟钻),Hong-Fu Wang(王洪福), and Shou Zhang(张寿)

Citation: Chin. Phys. B, 2023, 32 (**11**): 110307. DOI: 10.1088/1674-1056/acdc0f
Journal homepage: http://cpb.iphy.ac.cn; http://iopscience.iop.org/cpb

What follows is a list of articles you may be interested in

Deterministic remote state preparation of arbitrary three-qubit state through noisy cluster-GHZ channel

Zhihang Xu(许智航), Yuzhen Wei(魏玉震), Cong Jiang(江聪), and Min Jiang(姜敏)
Chin. Phys. B, 2022, 31 (**4**): 040304. DOI: 10.1088/1674-1056/ac2b17

Quantum multicast schemes of different quantum states via non-maximally entangled channels with multiparty involvement

Yan Yu(于妍), Nan Zhao(赵楠), Chang-Xing Pei(裴昌幸), and Wei Li(李玮)
Chin. Phys. B, 2021, 30 (**9**): 090302. DOI: 10.1088/1674-1056/abeef2

Efficient scheme for remote preparation of arbitrary *n*-qubit equatorial states

Xin-Wei Zha(查新未), Min-Rui Wang(王敏锐), Ruo-Xu Jiang(姜若虚)
Chin. Phys. B, 2020, 29 (**4**): 040304. DOI: 10.1088/1674-1056/ab773d

Deterministic hierarchical joint remote state preparation with six-particle partially entangled state

Na Chen(陈娜), Bin Yan(颜斌), Geng Chen(陈赓), Man-Jun Zhang(张曼君), Chang-Xing Pei(裴昌幸)
Chin. Phys. B, 2018, 27 (**9**): 090304. DOI: 10.1088/1674-1056/27/9/090304

Controlled remote preparation of an arbitrary four-qubit cluster-type state

Wei-Lin Chen(陈维林), Song-Ya Ma(马松雅), Zhi-Guo Qu(瞿治国)
Chin. Phys. B, 2016, 25 (**10**): 100304. DOI: 10.1088/1674-1056/25/10/100304

Deterministic remote preparation of multi-qubit equatorial states through dissipative channels

Liu-Yong Cheng(程留永)[1,†], Shi-Feng Zhang(张世凤)[1], Zuan Meng(孟钻)[1], Hong-Fu Wang(王洪福)[2], and Shou Zhang(张寿)[2]

[1] *School of Physics and Information Engineering, Shanxi Normal University, Taiyuan* 030031, *China*
[2] *Department of Physics, College of Science, Yanbian University, Yanji* 133002, *China*

(Received 25 February 2023; revised manuscript received 10 May 2023; accepted manuscript online 7 June 2023)

We investigate the influence of a noisy environment on the remote preparation of the multi-qubit equatorial state, and specifically deduce the final states and fidelities of the remote preparation of the three-qubit and four-qubit equatorial states under diverse types of noisy environments, namely, amplitude damping, bit flip, phase damping, phase flip, bit-phase flip, depolarization, and non-Markov environments. The results show that when the decoherence factors of the front six noises are equal, the influence degrees of phase damped noise, bit flip noise, phase flip noise, and bit-phase flip noise are similar, while the information loss caused by the amplitude damped noise and depolarizing noise is less. In particular, the bit flip noise and depolarizing noise may have more complex effects on the remote state preparation (RSP) schemes depending on the phase information of the target states, even for the ideal cases where the fidelity values are always 1 for specific phase relations. In the non-Markov environment, owing to the back and forth of information between the environment and systems, fidelities exhibit oscillating behavior and the minimum value may stay greater than zero for a long evolutionary time. These results are expected to have potential applications for understanding and avoiding the influence of noise on remote quantum communication and quantum networks.

Keywords: remote state preparation, dissipative channel, equatorial state, fidelity

PACS: 03.67.–a, 03.67.Hk, 03.65.Ud **DOI:** 10.1088/1674-1056/acdc0f

1. Introduction

Quantum communication and quantum information technology demonstrate prominent advantages in many modern information processing tasks with enhanced security, fast speed, and high transmission efficiency. As a unique resource, quantum entanglement has been widely used in many quantum information processing protocols, such as quantum teleportation (QT),[1,2] quantum secret sharing,[3,4] quantum secure direct communication (QSDC),[5–8] and remote state preparation (RSP).[9–11] Quantum teleportation is a typical quantum process that allows one to send an unknown quantum state to another one through local operations and classical communication (LOCC) without physically transporting particles. Remote state preparation is another unique quantum process, in contrast to QT, which is used to transmit a known state between sender and receiver. Therefore, RSP schemes consume less qubit resources. So far, RSP has gained extensive interest and research, such as deterministic RSP (DRSP),[12,13] joint RSP (JRSP),[14–18] controlled RSP (CRSP),[19–25] and continuous variable RSP.[26,27] Several RSP programs have been experimentally implemented in linear optical systems,[28] cavity QED,[29–31] and nuclear magnetic resonance systems.[32] However, in long-distance quantum communication, quantum states or quantum channels inevitably interact with the external environment, and environmental noise and noise-induced decoherence may lead to deviations in quantum information processing tasks. In actual quantum communication, five types of noise are often encountered, which are amplitude damping noise, phase damping noise, bit flip noise, phase flip noise, and depolarizing noise.[33] Remote state preparation schemes in noisy environments have also been studied.[34–42]

Equatorial state is a special class of quantum states of the Bloch sphere. In contrast to general quantum states, some of the equatorial state's information is known. So they have some special properties and are easy to prepare. These quantum states have many specific applications in quantum information processing, such as remote realization of unitary operations,[43,44] and phase-covariant quantum cloning machines.[45–47] In recent years, remote preparation of equatorial states has been proposed. In 2011, Chen *et al.* proposed probabilistic joint remote preparation of two-particle high-dimensional equatorial states.[48] Choudhury *et al.* proposed a JRSP scheme for preparing two-qubit equatorial states in 2015.[49] In the same year, Li *et al.* proposed a joint remote preparation scheme of multi-qubit equatorial states.[50] In 2017, Adepoju *et al.* proposed a JRSP scheme of two-qubit equatorial state in noisy channels.[51] In 2018, Sun *et al.* proposed an asymmetric controllable bidirectional JRSP method for single-qubit and three-qubit equatorial states in a noisy environment.[52] In the same year, Wei *et al.* proposed a DRSP scheme of arbitrary multi-qubit equatorial states.[53]

[†]Corresponding author. E-mail: lycheng@sxnu.edu.cn

© 2023 Chinese Physical Society and IOP Publishing Ltd

Later, Sun *et al.* realized asymmetric synchronous bidirectional transmission of equatorial states.[54,55] In 2020, Zha *et al.* proposed the remote deterministic preparation of arbitrary n qubit equatorial states using the maximally entangled state channel.[56] Very recently, Wang *et al.* proposed bidirectional three-qubit and four-qubit CRSP schemes.[57]

It should be noted that there are few comprehensive studies on the remote preparation of multi-qubit equatorial states in a noisy environment. To our knowledge, Adepoju *et al.* proposed a JRSP scheme of two-qubit equatorial state for six noisy channels in 2017.[51] Subsequently, Sun *et al.* proposed an asymmetric controllable bidirectional JRSP method for single-qubit and three-qubit equatorial states in a noisy environment with nine-qubit entangled state as the quantum channel.[52] Here, we investigate the effect of diverse quantum noises on the RSP of multi-qubit equatorial states with Bell state channels. The effects of amplitude damping noise, phase damping noise, bit flip noise, phase flip noise, bit-phase flip noise, depolarizing noise, and non-Markov environmental noise on the remote preparation of three-qubit and four-qubit equatorial states are analyzed in detail. The fidelities of the final states are quantitatively analyzed. The results show that the fidelities are related to the noise factors and the parameters of equatorial states. A comparative analysis shows that there are many differences in the influence of different noises on the state preparation. This makes it possible to better understand the influence of ambient noise on RSP and distributed quantum communication networks.

This article is organized as follows. In Section 2, we review the RSP of multi-qubit equatorial states under ideal conditions. Then, in Sections 3, 4, and 5, the three-qubit and four-qubit equatorial states are taken as examples to expound the influence of environmental noise on the remote preparation of expected states. Finally, our discussions and conclusions are given in Section 6.

2. Remote state preparation of general multi-qubit equatorial states

We first introduce the RSP process without considering noise. Suppose that there are two spatially distant participants, Alice and Bob. Alice wants to help Bob prepare a general n-qubit equatorial state in form of

$$|\chi\rangle = \frac{1}{\sqrt{2^n}} \sum_{j=0}^{2^n-1} (\mathrm{e}^{\mathrm{i}\theta_j} |a_n \cdots a_2 a_1\rangle), \tag{1}$$

where $a_l \in \{0,1\}$, $0 \le \theta_j \le 2\pi$, $j = \sum_{l=1}^{n} a_l \cdot 2^{l-1}$ is the corresponding decimal number of binary string $a_n \cdots a_2 a_1$. Initially, Alice and Bob share n sets of two-qubit maximally entangled Bell states as quantum channels. The channels can be expressed as

$$|\psi\rangle_{\mathrm{A}_n\mathrm{B}_n} = \bigotimes_{i=1}^{n} \left(\frac{1}{\sqrt{2}} |00\rangle_{\mathrm{A}_i\mathrm{B}_i} + \frac{1}{\sqrt{2}} |11\rangle_{\mathrm{A}_i\mathrm{B}_i} \right), \tag{2}$$

where particles belonging to Alice have subscript A and particles belonging to Bob have subscript B. According to the conventional RSP process, Alice needs to perform n-qubit projection measurement using a set of orthogonal measurement basis $\{|\Gamma_d\rangle,\ d = 1,2,\ldots,2^n\}$ to help Bob prepare the target state. Under this set of measurement basis, the entangled state of the entire system can be rewritten as

$$\begin{aligned} &|\psi\rangle_{\mathrm{A}_1\mathrm{B}_1} \otimes |\psi\rangle_{\mathrm{A}_2\mathrm{B}_2} \cdots \otimes |\psi\rangle_{\mathrm{A}_n\mathrm{B}_n} \\ &= \frac{1}{n} \left(|\Gamma_1\rangle_{\mathrm{A}_1\cdots\mathrm{A}_n} |\phi_1\rangle_{\mathrm{B}_1\cdots\mathrm{B}_n} + \cdots + |\Gamma_{2^n}\rangle_{\mathrm{A}_1\cdots\mathrm{A}_n} |\phi_{2^n}\rangle_{\mathrm{B}_1\cdots\mathrm{B}_n} \right). \end{aligned} \tag{3}$$

After Alice completes the projection measurement of the particles in her hand, she announces the measurement results through classical channel. According to Alice's measurement results, Bob can perform the corresponding unitary operations to achieve the target state to be prepared.

It should be pointed out that the form of Alice's measurement basis is not unique theoretically. For instance, the measurement basis $\{|\Gamma_d\rangle\}$ can take the form of[56]

$$\begin{aligned} |\Gamma_1\rangle_{\mathrm{A}_1\cdots\mathrm{A}_n} &= I_{\mathrm{A}_1} \otimes I_{\mathrm{A}_2} \otimes I_{\mathrm{A}_3} \otimes \cdots \otimes I_{\mathrm{A}_n} |\Gamma_1\rangle_{\mathrm{A}_1\cdots\mathrm{A}_n}, \\ |\Gamma_2\rangle_{\mathrm{A}_1\cdots\mathrm{A}_n} &= \sigma_{\mathrm{A}_{1z}} \otimes I_{\mathrm{A}_2} \otimes I_{\mathrm{A}_3} \otimes \cdots \otimes I_{\mathrm{A}_n} |\Gamma_1\rangle_{\mathrm{A}_1\cdots\mathrm{A}_n}, \\ |\Gamma_3\rangle_{\mathrm{A}_1\cdots\mathrm{A}_n} &= I_{\mathrm{A}_1} \otimes \sigma_{\mathrm{A}_{2z}} \otimes I_{\mathrm{A}_3} \otimes \cdots \otimes I_{\mathrm{A}_n} |\Gamma_1\rangle_{\mathrm{A}_1\cdots\mathrm{A}_n}, \\ &\vdots \\ |\Gamma_{2^n}\rangle_{\mathrm{A}_1\cdots\mathrm{A}_n} &= \sigma_{\mathrm{A}_{1z}} \otimes \sigma_{\mathrm{A}_{2z}} \otimes \sigma_{\mathrm{A}_{3z}} \otimes \cdots \otimes \sigma_{\mathrm{A}_{nz}} |\Gamma_1\rangle_{\mathrm{A}_1\cdots\mathrm{A}_n}, \end{aligned} \tag{4}$$

or the form of[53]

$$|\Gamma_d\rangle_{\mathrm{A}_1\cdots\mathrm{A}_n} = \frac{1}{\sqrt{2^n}} \sum_{j=0}^{2^n-1} \left[\exp\left(\frac{\mathrm{i}\pi jd}{2^n - 1} - \mathrm{i}\theta_j \right) |a_n \cdots a_2 a_1\rangle \right]. \tag{5}$$

Taking the first form of measurement basis as an example, if Alice's measurement result is $|\Gamma_{2^n}\rangle_{\mathrm{A}_1\cdots\mathrm{A}_n}$, then Bob's particles will collapse into state $|\phi_{2^n}\rangle_{\mathrm{B}_1\cdots\mathrm{B}_n}$. Bob can then perform appropriate unitary operations $\sigma_{\mathrm{B}_{1z}} \otimes \sigma_{\mathrm{B}_{2z}} \otimes \sigma_{\mathrm{B}_{3z}} \otimes \cdots \otimes \sigma_{\mathrm{B}_{nz}}$ on the particles in his hand to realize the target state $|\chi\rangle$.

However, in a practical communication process, a quantum system will inevitably interact with the environment. The environmental noise will have a certain impact on the success or performance of the quantum communication schemes. Therefore, it is instructive to research the effect of quantum noise on the RSP process. Here, we first study the influence of six common quantum noises, which are amplitude damping noise, bit flip noise, phase damping noise, phase flip noise, bit-phase flip noise, and depolarizing noise, followed by the analysis of non-Markovian effects on the RSP schemes. The effects of quantum noises can be mathematically regarded as some specific kinds of quantum operation, expressed in the

form of corresponding operators. In addition, we can determine the information loss due to noise during RSP by calculating the fidelity of the obtained state. The formula for calculating the fidelity of the final system is

$$F = \langle\chi|\rho_{\text{out}}|\chi\rangle. \tag{6}$$

The fidelity ranges from 0 to 1 and the smaller F means more information is lost in a noisy environment. Next, we will illustrate the RSP processes of three-qubit and four-qubit equatorial states in different kinds of noisy environment and deduce the fidelity of the final states.

3. RSP of three-qubit equatorial states in common noisy environments

To elaborate the influence of environmental noise on the RSP of multi-qubit equatorial states, we begin to take the three-qubit equatorial state as an example. Here, Alice wants to help Bob remotely prepare the three-qubit equatorial state expressed as

$$\begin{aligned}|\chi\rangle \;=\; & \frac{1}{2\sqrt{2}}(\mathrm{e}^{\mathrm{i}\theta_0}|000\rangle + \mathrm{e}^{\mathrm{i}\theta_1}|001\rangle + \mathrm{e}^{\mathrm{i}\theta_2}|010\rangle + \mathrm{e}^{\mathrm{i}\theta_3}|011\rangle \\ & + \mathrm{e}^{\mathrm{i}\theta_4}|100\rangle + \mathrm{e}^{\mathrm{i}\theta_5}|101\rangle + \mathrm{e}^{\mathrm{i}\theta_6}|110\rangle + \mathrm{e}^{\mathrm{i}\theta_7}|111\rangle).\end{aligned} \tag{7}$$

The quantum channels between Alice and Bob are three two-qubit entangled Bell states

$$\begin{aligned}|\Psi\rangle_{\mathrm{A_1A_2A_3B_1B_2B_3}} \;=\; & \frac{1}{2\sqrt{2}}(|00\rangle_{\mathrm{A_1B_1}} + |11\rangle_{\mathrm{A_1B_1}}) \\ & \otimes(|00\rangle_{\mathrm{A_2B_2}} + |11\rangle_{\mathrm{A_2B_2}}) \\ & \otimes(|00\rangle_{\mathrm{A_3B_3}} + |11\rangle_{\mathrm{A_3B_3}}).\end{aligned} \tag{8}$$

Consider that Bob is the generator of the entangled resource $|\Psi\rangle_{\mathrm{A_1A_2A_3B_1B_2B_3}}$. He keeps the particles $\{\mathrm{B_1},\ \mathrm{B_2},\ \mathrm{B_3}\}$ and sends the particles $\{\mathrm{A_1},\ \mathrm{A_2},\ \mathrm{A_3}\}$ to Alice through the noisy channel. Therefore, in the subsequent RSP process, we only consider the influence of noise on particles $\{\mathrm{A_1},\ \mathrm{A_2},\ \mathrm{A_3}\}$. For simplicity, we assume that all particles experience the identical noise.

3.1. The amplitude damping noise

The amplitude damping noise can be used to describe the energy dissipation effects due to energy loss in a quantum system. In quantum optics, the spontaneous radiation of a two-level atom from excited state to ground state and the decay of a single photon from a micro-cavity can be described by this noise mechanism. The general behavior of amplitude damping noise can be represented by the following Kraus operators:

$$E_0 = \begin{pmatrix} 1 & 0 \\ 0 & \sqrt{1-\kappa} \end{pmatrix},\ E_1 = \begin{pmatrix} 1 & \sqrt{\kappa} \\ 0 & 0 \end{pmatrix}, \tag{9}$$

where κ indicates the decoherence rate of amplitude damping noise. In such a noisy transmission environment, the density matrix of quantum system evolves as $\rho \to \varepsilon(\rho) = E_0^{\dagger}\rho E_0 + E_1^{\dagger}\rho E_1$.

Under the influence of amplitude damping noise, the quantum channels between Alice and Bob evolve as

$$\begin{aligned}&\xi_{\mathrm{A_1A_2A_3B_1B_2B_3}}(\rho) \\ =\; & \frac{1}{8-12\kappa+6\kappa^2}\{[|000000\rangle + (1-\kappa)^{\frac{1}{2}}|001001\rangle \\ & +(1-\kappa)^{\frac{1}{2}}|010010\rangle + (1-\kappa)|011011\rangle + (1-\kappa)^{\frac{1}{2}}|100100\rangle \\ & +(1-\kappa)|101101\rangle + (1-\kappa)|110110\rangle + (1-\kappa)^{\frac{3}{2}}|111111\rangle] \\ & \otimes[\langle 000000| + (1-\kappa)^{\frac{1}{2}}\langle 001001| + (1-\kappa)^{\frac{1}{2}}\langle 010010| \\ & +(1-\kappa)\langle 011011| + (1-\kappa)^{\frac{1}{2}}\langle 100100| + (1-\kappa)\langle 101101| \\ & +(1-\kappa)\langle 110110| + (1-\kappa)^{\frac{3}{2}}\langle 111111|] \\ & +\kappa^3|000111\rangle\langle 000111|\}.\end{aligned} \tag{10}$$

The density matrix of the final state after Alice's measurements and Bob's unitary operations becomes

$$\begin{aligned}&\rho_{\mathrm{outB_1B_2B_3}} \\ =\; & \frac{1}{8-12\kappa+6\kappa^2}\{[\mathrm{e}^{\mathrm{i}\theta_0}|000\rangle + (1-\kappa)^{\frac{1}{2}}\mathrm{e}^{\mathrm{i}\theta_1}|001\rangle \\ & +(1-\kappa)^{\frac{1}{2}}\mathrm{e}^{\mathrm{i}\theta_2}|010\rangle + (1-\kappa)\mathrm{e}^{\mathrm{i}\theta_3}|011\rangle \\ & +(1-\kappa)^{\frac{1}{2}}\mathrm{e}^{\mathrm{i}\theta_4}|100\rangle + (1-\kappa)\mathrm{e}^{\mathrm{i}\theta_5}|101\rangle \\ & +(1-\kappa)\mathrm{e}^{\mathrm{i}\theta_6}|110\rangle + (1-\kappa)^{\frac{3}{2}}\mathrm{e}^{\mathrm{i}\theta_7}|111\rangle] \\ & \otimes[\mathrm{e}^{-\mathrm{i}\theta_0}\langle 000| + (1-\kappa)^{\frac{1}{2}}\mathrm{e}^{-\mathrm{i}\theta_1}\langle 001| + (1-\kappa)^{\frac{1}{2}}\mathrm{e}^{-\mathrm{i}\theta_2}\langle 010| \\ & +(1-\kappa)\mathrm{e}^{-\mathrm{i}\theta_3}\langle 011| + (1-\kappa)^{\frac{1}{2}}\mathrm{e}^{-\mathrm{i}\theta_4}\langle 100| \\ & +(1-\kappa)\mathrm{e}^{-\mathrm{i}\theta_5}\langle 101| + (1-\kappa)\mathrm{e}^{-\mathrm{i}\theta_6}\langle 110| \\ & +(1-\kappa)^{\frac{3}{2}}\mathrm{e}^{-\mathrm{i}\theta_7}\langle 111|] + \kappa^3|111\rangle\langle 111|\}.\end{aligned} \tag{11}$$

The explicit measurement results of Alice and the corresponding unitary operations of Bob are given in Appendix A.

We can then calculate the fidelity of the final state under the influence of amplitude damping noise as

$$\begin{aligned}F \;=\; & \frac{1}{8(8-12\kappa+6\kappa^2)}\{[1+3(1-\kappa)^{\frac{1}{2}} \\ & +3(1-\kappa)+(1-\kappa)^{\frac{3}{2}}]^2 + \kappa^3\}.\end{aligned} \tag{12}$$

It can be seen directly from Eq. (12) that the fidelity of state preparation depends on the decoherence rate of noise. And when $\kappa = 0$, $F = 1$, corresponding to the perfect preparation process under ideal environment. The specific relationship between fidelity and decoherence rate is shown in Fig. 1. As can be seen from the figure, the fidelity decreases as κ increases, and the decline rate is slow at first and is then fast, which show that the amplitude damping channel has a great influence on the results of the RSP. When $\kappa = 1$, the fidelity reached the minimum value of $1/8$.

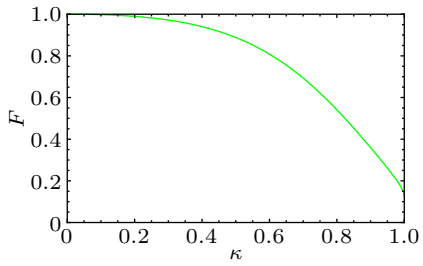


Fig. 1. The fidelity of RSP of three-qubit equatorial state with decoherence rate κ in amplitude damping noise.

3.2. The bit flip noise

The Kraus operators of bit flip noise can be represented as

$$E_0 = \sqrt{1-\lambda}\begin{pmatrix} 1 & 0 \\ 0 & 1 \end{pmatrix}, \quad E_1 = \sqrt{\lambda}\begin{pmatrix} 0 & 1 \\ 1 & 0 \end{pmatrix}, \tag{13}$$

where λ indicates the decoherence rate of bit flip noise. The physical effect of bit flip noise is to change a qubit state as $|0\rangle \to |1\rangle$ or $|1\rangle \to |0\rangle$ with the probability λ. In such a noisy transmission environment, the quantum channels between Alice and Bob evolve into

$$\begin{aligned}
&\xi_{A_1A_2A_3B_1B_2B_3}(\rho) \\
&= \frac{1}{8(1-\lambda)^3+8\lambda^3}[(1-\lambda)^{\frac{3}{2}}(|000000\rangle+|001001\rangle \\
&+|010010\rangle+|011011\rangle+|100100\rangle \\
&+|101101\rangle+|110110\rangle+|111111\rangle) \\
&\otimes(1-\lambda)^{\frac{3}{2}}(\langle 000000|+\langle 001001|+\langle 010010|+\langle 011011| \\
&+\langle 100100|+\langle 101101|+\langle 110110|+\langle 111111|) \\
&+\lambda^{\frac{3}{2}}(|111000\rangle+|110001\rangle+|101010\rangle+|100011\rangle \\
&+|011100\rangle+|010101\rangle+|001110\rangle+|000111\rangle) \\
&\otimes\lambda^{\frac{3}{2}}(\langle 111000|+\langle 110001|+\langle 101010|+\langle 100011| \\
&+\langle 011100|+\langle 010101|+\langle 001110|+\langle 000111|)].
\end{aligned} \tag{14}$$

As a result, the density matrix of the final state obtained by the remote preparation of the three-qubit equatorial state becomes

$$\begin{aligned}
&\rho_{\mathrm{out}B_1B_2B_3} \\
&= \frac{1}{8(1-\lambda)^3+8\lambda^3}[(1-\lambda)^{\frac{3}{2}}(e^{i\theta_0}|000\rangle+e^{i\theta_1}|001\rangle \\
&+e^{i\theta_2}|010\rangle+e^{i\theta_3}|011\rangle+e^{i\theta_4}|100\rangle+e^{i\theta_5}|101\rangle \\
&+e^{i\theta_6}|110\rangle+e^{i\theta_7}|111\rangle) \\
&\otimes(1-\lambda)^{\frac{3}{2}}(e^{-i\theta_0}\langle 000|+e^{-i\theta_1}\langle 001|+e^{-i\theta_2}\langle 010| \\
&+e^{-i\theta_3}\langle 011|+e^{-i\theta_4}\langle 100|+e^{-i\theta_5}\langle 101| \\
&+e^{-i\theta_6}\langle 110|+e^{-i\theta_7}\langle 111|) \\
&+\lambda^{\frac{3}{2}}(e^{i\theta_7}|000\rangle+e^{i\theta_6}|001\rangle+e^{i\theta_5}|010\rangle+e^{i\theta_4}|011\rangle \\
&+e^{i\theta_3}|100\rangle+e^{i\theta_2}|101\rangle+e^{i\theta_1}|110\rangle+e^{i\theta_0}|111\rangle) \\
&\otimes\lambda^{\frac{3}{2}}(e^{-i\theta_7}\langle 000|+e^{-i\theta_6}\langle 001|+e^{-i\theta_5}\langle 010| \\
&+e^{-i\theta_4}\langle 011|+e^{-i\theta_3}\langle 100|+e^{-i\theta_2}\langle 101| \\
&+e^{-i\theta_1}\langle 110|+e^{-i\theta_0}\langle 111|)].
\end{aligned} \tag{15}$$

The fidelity of the final state under the influence of bit flip noise is

$$\begin{aligned}
F = &\frac{1}{(1-\lambda)^3+\lambda^3}\{(1-\lambda)^3+\frac{1}{16}\lambda^3[\cos(\theta_7-\theta_0) \\
&+\cos(\theta_6-\theta_1)+\cos(\theta_5-\theta_2)+\cos(\theta_4-\theta_3)]^2\}.
\end{aligned} \tag{16}$$

As can be seen from the above formula, the fidelity of state preparation under bit flip noise is related not only to the noise factor but also to the phase information of the target state. To unambiguously analyze the relationship between fidelity and the noise factor, we choose $\theta_7-\theta_0=\theta_6-\theta_1=\theta_5-\theta_2=\theta_4-\theta_3=\theta$. Figure 2(a) gives two-dimensional diagrams of fidelity changing with noise factor λ when $\theta=\pi/4$, $\pi/2$ and π, respectively. As shown in the figure, when $\theta=\pi/4$ or $\pi/2$, the fidelity value has three changing stages as slow decrease, dramatic decrease, and gentle change for the noise factor intervals $0<\lambda<0.3$, $0.3<\lambda<0.6$ and $0.6<\lambda<1$, and gets the minimum value 0.5 or 0 for $\lambda=1$. But when $\theta=\pi$ (or integer multiples of π), no matter how the noise factor changes, the fidelity is always equal to 1, so that the remote state preparation is not affected by the bit flip noise for target states with this special phase relationship.

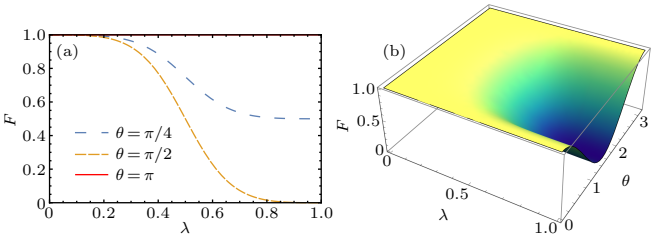


Fig. 2. (a) The fidelity of RSP of three-qubit equatorial state with decoherence rate λ in bit flip noise for $\theta=\pi/4$, $\pi/2$ and π. (b) The fidelity of RSP of three-qubit equatorial state with decoherence rate λ and phase parameter θ in bit flip noise.

To show the relationship between decoherence rate, phase information of equatorial state, and fidelity of final state more visually, in Fig. 2(b), we demonstrate the three-dimensional diagram of bit flip noise λ, phase information θ, and fidelity F. As can be seen, the remote preparation fidelity of equatorial states with different phase relationships is not the same in the bit flip noise environment, especially when the noise factor is large. Furthermore, for the same λ value, the fidelity curve has a rising-falling turning point at $\theta=\pi/2$ ($F=0$) in $0<\theta<\pi$. This is due to the periodic property of the cosine function in the fidelity Eq. (16).

3.3. The phase damping noise

In contrast to amplitude damping noise, phase damping noise describes the interaction of quantum system with the surrounding environment when no energy loss is involved. The behavior of this noise can be characterized by the following Kraus operators:

$$E_0=\sqrt{1-\mu}\begin{pmatrix}1&0\\0&1\end{pmatrix},\ E_1=\sqrt{\mu}\begin{pmatrix}1&0\\0&0\end{pmatrix},$$
$$E_2=\sqrt{\mu}\begin{pmatrix}0&0\\0&1\end{pmatrix}, \tag{17}$$

where μ indicates the decoherence rate of phase damping noise. In such a noisy transmission environment, the density matrix of quantum system evolves as $\rho\to\varepsilon(\rho)=E_0^\dagger\rho E_0+E_1^\dagger\rho E_1+E_2^\dagger\rho E_2$.

Therefore, under the influence of phase damping noise, the quantum channels between Alice and Bob evolve as

$$\begin{aligned}&\xi_{A_1A_2A_3B_1B_2B_3}(\rho)\\&=\frac{1}{8(1-\mu)^3+2\mu^3}[(1-\mu)^{\frac{3}{2}}(|000000\rangle+|001001\rangle\\&+|010010\rangle+|011011\rangle+|100100\rangle\\&+(1-\mu)|101101\rangle+|110110\rangle+|111111\rangle)\\&\otimes(1-\mu)^{\frac{3}{2}}(\langle000000|+\langle001001|+\langle010010|+\langle011011|\\&+\langle100100|+\langle101101|+\langle110110|+\langle111111|)\\&+\mu^3|000000\rangle\langle000000|+\mu^3|111111\rangle\langle111111|].\end{aligned} \tag{18}$$

After Alice's projection measurements, the density matrix of the final state obtained by Bob becomes

$$\begin{aligned}&\rho_{outB_1B_2B_3}\\&=\frac{1}{8(1-\mu)^3+2\mu^3}[(1-\mu)^{\frac{3}{2}}(e^{i\theta_0}|000\rangle+e^{i\theta_1}|001\rangle\\&+e^{i\theta_2}|010\rangle+e^{i\theta_3}|011\rangle+e^{i\theta_4}|100\rangle+e^{i\theta_5}|101\rangle\\&+e^{i\theta_6}|110\rangle+e^{i\theta_7}|111\rangle)\\&\otimes(1-\mu)^{\frac{3}{2}}(e^{-i\theta_0}\langle000|+e^{-i\theta_1}\langle001|+e^{-i\theta_2}\langle010|\\&+e^{-i\theta_3}\langle011|+e^{-i\theta_4}\langle100|+e^{-i\theta_5}\langle101|+e^{-i\theta_6}\langle110|\\&+e^{-i\theta_7}\langle111|)+\mu^3|000\rangle\langle000|+\mu^3|111\rangle\langle111|].\end{aligned} \tag{19}$$

We can calculate the fidelity of the final state under the influence of phase damping noise as

$$F=\frac{1}{8(1-\mu)^3+2\mu^3}\left[8(1-\mu)^3+\frac{1}{4}\mu^3\right]. \tag{20}$$

Figure 3 shows the relationship between decoherence rate μ and fidelity in the phase damping noise environment. As can be seen from Eq. (20) and Fig. 3, the fidelity depends on the decoherence rate μ. When $\mu=0$, the maximum fidelity is 1, and the fidelity gradually decreases with the increase of μ. Specifically, the fidelity decreases slowly with the increase of μ in $0<\mu<0.4$, decreases rapidly in $0.4<\mu<0.8$ and becomes less steep in $0.8<\mu<1$. When $\mu=1$, the fidelity reaches the minimum value of $1/8$.

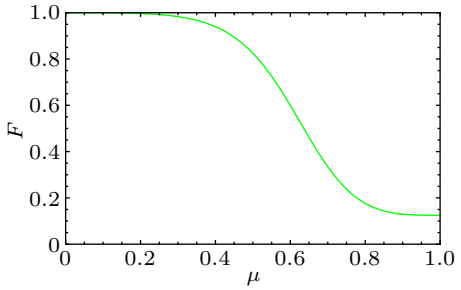


Fig. 3. The fidelity of RSP of three-qubit equatorial state with decoherence rate μ in phase damping noise.

3.4. The phase flip noise

The Kraus operators of phase flip noise can be represented as

$$E_0=\sqrt{1-\eta}\begin{pmatrix}1&0\\0&1\end{pmatrix},\ E_1=\sqrt{\eta}\begin{pmatrix}1&0\\0&-1\end{pmatrix}, \tag{21}$$

where η indicates the decoherence rate of phase flip noise. In the phase flip noise environment, the quantum channels between Alice and Bob evolve into

$$\begin{aligned}&\xi_{A_1A_2A_3B_1B_2B_3}(\rho)\\&=\frac{1}{8(1-\eta)^3+8\eta^3}[(1-\eta)^{\frac{3}{2}}(|000000\rangle+|001001\rangle\\&+|010010\rangle+|011011\rangle+|100100\rangle+|101101\rangle\\&+|110110\rangle+|111111\rangle)\\&\otimes(1-\eta)^{\frac{3}{2}}(\langle000000|+\langle001001|+\langle010010|+\langle011011|\\&+\langle100100|+\langle101101|+\langle110110|+\langle111111|)\\&+\eta^{\frac{3}{2}}(|000000\rangle-|001001\rangle-|010010\rangle+|011011\rangle\\&-|110100\rangle+|101101\rangle+|110110\rangle-|111111\rangle)\\&\otimes\eta^{\frac{3}{2}}(\langle000000|-\langle001001|-\langle010010|+\langle011011|\\&-\langle100100|+\langle101101|+\langle110110|-\langle111111|)].\end{aligned} \tag{22}$$

After Alice's measurements, the density matrix of the final state obtained by Bob becomes

$$\begin{aligned}&\rho_{outB_1B_2B_3}\\&=\frac{1}{8(1-\eta)^3+8\eta^3}[(1-\eta)^{\frac{3}{2}}(e^{i\theta_0}|000\rangle+e^{i\theta_1}|001\rangle\\&+e^{i\theta_2}|010\rangle+e^{i\theta_3}|011\rangle+e^{i\theta_4}|100\rangle+e^{i\theta_5}|101\rangle\\&+e^{i\theta_6}|110\rangle+e^{i\theta_7}|111\rangle)\\&\otimes(1-\eta)^{\frac{3}{2}}(e^{-i\theta_0}\langle000|+e^{-i\theta_1}\langle001|+e^{-i\theta_2}\langle010|\\&+e^{-i\theta_3}\langle011|+e^{-i\theta_4}\langle100|+e^{-i\theta_5}\langle101|\end{aligned}$$

$$
\begin{aligned}
&+\mathrm{e}^{-\mathrm{i}\theta_6}\langle 110|+\mathrm{e}^{-\mathrm{i}\theta_7}\langle 111|)\\
&+\eta^{\frac{3}{2}}(\mathrm{e}^{\mathrm{i}\theta_0}|000\rangle-\mathrm{e}^{\mathrm{i}\theta_1}|001\rangle-\mathrm{e}^{\mathrm{i}\theta_2}|010\rangle+\mathrm{e}^{\mathrm{i}\theta_3}|011\rangle\\
&-\mathrm{e}^{\mathrm{i}\theta_4}|100\rangle+\mathrm{e}^{\mathrm{i}\theta_5}|101\rangle+\mathrm{e}^{\mathrm{i}\theta_6}|110\rangle-\mathrm{e}^{\mathrm{i}\theta_7}|111\rangle)\\
&\otimes\eta^{\frac{3}{2}}(\mathrm{e}^{-\mathrm{i}\theta_0}\langle 000|-\mathrm{e}^{-\mathrm{i}\theta_1}\langle 001|-\mathrm{e}^{-\mathrm{i}\theta_2}\langle 010|\\
&+\mathrm{e}^{-\mathrm{i}\theta_3}\langle 011|-\mathrm{e}^{-\mathrm{i}\theta_4}\langle 100|+\mathrm{e}^{-\mathrm{i}\theta_5}\langle 101|\\
&+\mathrm{e}^{-\mathrm{i}\theta_6}\langle 110|-\mathrm{e}^{-\mathrm{i}\theta_7}\langle 111|)].
\end{aligned}
\tag{23}
$$

The fidelity of the final state under the influence of phase flip noise is

$$
F=\frac{(1-\eta)^3}{(1-\eta)^3+\eta^3}. \tag{24}
$$

Figure 4 is a two-dimensional diagram of fidelity changing with noise factor η. As can be seen, the fidelity gradually decreases with the increase of η. When $\eta=0$, the fidelity reaches the maximum value 1. When $0<\eta<0.3$, the fidelity decreases slowly with the increase of η and changes quickly in $0.3<\eta<0.7$. Finally, the fidelity gradually reaches 0 when $\eta=1$.

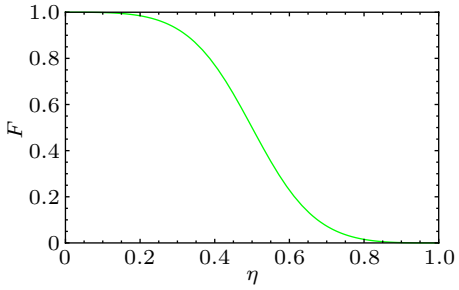


Fig. 4. The fidelity of RSP of three-qubit equatorial state with decoherence rate η in phase flip noise.

3.5. The depolarizing noise

The Kraus operators of depolarizing noise can be represented as

$$
\begin{aligned}
&E_0=\sqrt{1-\omega}\begin{pmatrix}1&0\\0&1\end{pmatrix},\ E_1=\sqrt{\omega/3}\begin{pmatrix}0&1\\1&0\end{pmatrix},\\
&E_2=\sqrt{\omega/3}\begin{pmatrix}0&-\mathrm{i}\\\mathrm{i}&0\end{pmatrix},\ E_3=\sqrt{\omega/3}\begin{pmatrix}1&0\\0&-1\end{pmatrix},
\end{aligned}
\tag{25}
$$

where ω indicates the decoherence rate of depolarizing noise. The physical effect of depolarizing noise is to keep the original state unchanged with probability $1-\omega$, and to have a bit flip, phase flip, or bit-phase flip with probability $\omega/3$, respectively. In such a noisy transmission environment, the quantum channels between Alice and Bob evolve into

$$
\begin{aligned}
&\xi_{\mathrm{A_1A_2A_3B_1B_2B_3}}(\rho)\\
&=\frac{1}{8(1-\omega)^3+8(\omega/3)^3}[(1-\omega)^{\frac{3}{2}}(|000000\rangle+|001001\rangle\\
&+|010010\rangle+|011011\rangle+|100100\rangle\\
&+|101101\rangle+|110110\rangle+|111111\rangle)\\
&\otimes(1-\omega)^{\frac{3}{2}}(\langle 000000|+\langle 001001|+\langle 010010|+\langle 011011|\\
&+\langle 100100|+\langle 101101|+\langle 110110|+\langle 111111|)\\
&+(\omega/3)^{\frac{3}{2}}(|111000\rangle+|110001\rangle+|101010\rangle+|100011\rangle\\
&+|011100\rangle+|010101\rangle+|001110\rangle+|000111\rangle)\\
&\otimes(\omega/3)^{\frac{3}{2}}(\langle 111000|+\langle 110001|+\langle 101010|+\langle 100011|\\
&+\langle 011100|+\langle 010101|+\langle 001110|+\langle 000111|)\\
&+(\omega/3)^{\frac{3}{2}}\mathrm{i}(|111000\rangle-|110001\rangle-|101010\rangle+|100011\rangle\\
&-|011100\rangle+|010101\rangle+|001110\rangle-|000111\rangle)\\
&\otimes(\omega/3)^{\frac{3}{2}}\mathrm{i}(\langle 111000|-\langle 110001|-\langle 101010|+\langle 100011|\\
&-\langle 011100|+\langle 010101|+\langle 001110|-\langle 000111|)\\
&+(\omega/3)^{\frac{3}{2}}(|000000\rangle-|001001\rangle-|010010\rangle+|100011\rangle\\
&-|100100\rangle+|101101\rangle+|110110\rangle-|111111\rangle)\\
&\otimes(\omega/3)^{\frac{3}{2}}(\langle 000000|-\langle 001001|-\langle 010010|+\langle 011011|\\
&-\langle 100100|+\langle 101101|+\langle 110110|-\langle 111111|)].
\end{aligned}
\tag{26}
$$

As a result, the density matrix of the final state obtained by the remote preparation of the three-qubit equatorial state becomes

$$
\begin{aligned}
&\rho_{\mathrm{outB_1B_2B_3}}\\
&=\frac{1}{8(1-\omega)^3+8(\omega/3)^3}[(1-\omega)^{\frac{3}{2}}(\mathrm{e}^{\mathrm{i}\theta_0}|000\rangle+\mathrm{e}^{\mathrm{i}\theta_1}|001\rangle\\
&+\mathrm{e}^{\mathrm{i}\theta_2}|010\rangle+\mathrm{e}^{\mathrm{i}\theta_3}|011\rangle+\mathrm{e}^{\mathrm{i}\theta_4}|100\rangle+\mathrm{e}^{\mathrm{i}\theta_5}|101\rangle\\
&+\mathrm{e}^{\mathrm{i}\theta_6}|110\rangle+\mathrm{e}^{\mathrm{i}\theta_7}|111\rangle)\\
&\otimes(1-\omega)^{\frac{3}{2}}(\mathrm{e}^{-\mathrm{i}\theta_0}\langle 000|+\mathrm{e}^{-\mathrm{i}\theta_1}\langle 001|+\mathrm{e}^{-\mathrm{i}\theta_2}\langle 010|\\
&+\mathrm{e}^{-\mathrm{i}\theta_3}\langle 011|+\mathrm{e}^{-\mathrm{i}\theta_4}\langle 100|+\mathrm{e}^{-\mathrm{i}\theta_5}\langle 101|\\
&+\mathrm{e}^{-\mathrm{i}\theta_6}\langle 110|+\mathrm{e}^{-\mathrm{i}\theta_7}\langle 111|)\\
&+(\omega/3)^{\frac{3}{2}}(\mathrm{e}^{\mathrm{i}\theta_7}|000\rangle+\mathrm{e}^{\mathrm{i}\theta_6}|001\rangle+\mathrm{e}^{\mathrm{i}\theta_5}|010\rangle+\mathrm{e}^{\mathrm{i}\theta_4}|011\rangle\\
&+\mathrm{e}^{\mathrm{i}\theta_3}|100\rangle+\mathrm{e}^{\mathrm{i}\theta_2}|101\rangle+\mathrm{e}^{\mathrm{i}\theta_1}|110\rangle+\mathrm{e}^{\mathrm{i}\theta_0}|111\rangle)\\
&\otimes(\omega/3)^{\frac{3}{2}}(\mathrm{e}^{-\mathrm{i}\theta_7}\langle 000|+\mathrm{e}^{-\mathrm{i}\theta_6}\langle 001|+\mathrm{e}^{-\mathrm{i}\theta_5}\langle 010|\\
&+\mathrm{e}^{-\mathrm{i}\theta_4}\langle 011|+\mathrm{e}^{-\mathrm{i}\theta_3}\langle 100|+\mathrm{e}^{-\mathrm{i}\theta_2}\langle 101|\\
&+\mathrm{e}^{-\mathrm{i}\theta_1}\langle 110|+\mathrm{e}^{-\mathrm{i}\theta_0}\langle 111|)\\
&+(\omega/3)^{\frac{3}{2}}\mathrm{i}(\mathrm{e}^{\mathrm{i}\theta_7}|000\rangle-\mathrm{e}^{\mathrm{i}\theta_6}|001\rangle-\mathrm{e}^{\mathrm{i}\theta_5}|010\rangle+\mathrm{e}^{\mathrm{i}\theta_4}|011\rangle\\
&-\mathrm{e}^{\mathrm{i}\theta_3}|100\rangle+\mathrm{e}^{\mathrm{i}\theta_2}|101\rangle+\mathrm{e}^{\mathrm{i}\theta_1}|110\rangle-\mathrm{e}^{\mathrm{i}\theta_0}|111\rangle)\\
&\otimes(\omega/3)^{\frac{3}{2}}\mathrm{i}(\mathrm{e}^{-\mathrm{i}\theta_7}\langle 000|-\mathrm{e}^{-\mathrm{i}\theta_6}\langle 001|-\mathrm{e}^{-\mathrm{i}\theta_5}\langle 010|\\
&+\mathrm{e}^{-\mathrm{i}\theta_4}\langle 011|-\mathrm{e}^{-\mathrm{i}\theta_3}\langle 100|+\mathrm{e}^{-\mathrm{i}\theta_2}\langle 101|+\mathrm{e}^{-\mathrm{i}\theta_1}\langle 110|\\
&-\mathrm{e}^{-\mathrm{i}\theta_0}\langle 111|)\\
&+(\omega/3)^{\frac{3}{2}}(\mathrm{e}^{\mathrm{i}\theta_0}|000\rangle-\mathrm{e}^{\mathrm{i}\theta_1}|001\rangle-\mathrm{e}^{\mathrm{i}\theta_2}|010\rangle+\mathrm{e}^{\mathrm{i}\theta_3}|011\rangle\\
&-\mathrm{e}^{\mathrm{i}\theta_4}|100\rangle+\mathrm{e}^{\mathrm{i}\theta_5}|101\rangle+\mathrm{e}^{\mathrm{i}\theta_6}|110\rangle-\mathrm{e}^{\mathrm{i}\theta_7}|111\rangle)
\end{aligned}
$$

$$\otimes(\omega/3)^{\frac{3}{2}}\left(\mathrm{e}^{-\mathrm{i}\theta_0}\langle 000|-\mathrm{e}^{-\mathrm{i}\theta_1}\langle 001|-\mathrm{e}^{-\mathrm{i}\theta_2}\langle 010|\right.$$
$$+\mathrm{e}^{-\mathrm{i}\theta_3}\langle 011|-\mathrm{e}^{-\mathrm{i}\theta_4}\langle 100|+\mathrm{e}^{-\mathrm{i}\theta_5}\langle 101|$$
$$\left.+\mathrm{e}^{-\mathrm{i}\theta_6}\langle 110|-\mathrm{e}^{-\mathrm{i}\theta_7}\langle 111|\right)]. \tag{27}$$

The fidelity of the final state under the influence of depolarizing noise is

$$F = \frac{1}{(1-\omega)^3+(\omega/3)^3}\left\{(1-\omega)^3+\frac{1}{16}(\omega/3)^3\right.$$
$$\times\left[\cos(\theta_7-\theta_0)+\cos(\theta_6-\theta_1)+\cos(\theta_5-\theta_2)\right.$$
$$\left.+\cos(\theta_4-\theta_3)\right]^2-\left[\sin(\theta_7-\theta_0)-\sin(\theta_6-\theta_1)\right.$$
$$\left.\left.-\sin(\theta_5-\theta_2)+\sin(\theta_4-\theta_3)\right]^2\right\}. \tag{28}$$

The fidelity of state preparation under depolarizing noise is related not only to the noise factor but also to the phase information of the target state. For simplicity, we first choose $\theta_7-\theta_0=\theta_6-\theta_1=\theta_5-\theta_2=\theta_4-\theta_3=\theta$ to analyze the relationship between fidelity and the noise factor. Figure 5(a) gives two-dimensional diagrams of fidelity changing with noise factor ω when $\theta=\pi/4$, $\pi/2$ and π, respectively. As shown in the figure, when $\theta=\pi/4$ or $\pi/2$, the fidelity value gradually decreases with the increase of ω and gets the minimum value 0.5 or 0 for $\omega=1$. And when $\omega=\pi$ (or integer multiples of π), no matter how the noise factor changes, the fidelity is always equal to 1. We show the three-dimensional relationship between fidelity, depolarizing noise factor ω, and phase factor θ in Fig. 5(b). The results shown in the figure are similar to the results shown in Fig. 2(b).

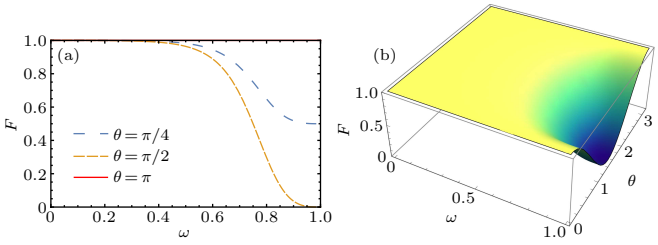


Fig. 5. (a) The fidelity of RSP of three-qubit equatorial state with decoherence rate ω in depolarizing noise for $\theta=\pi/4$, $\pi/2$ and π. (b) The fidelity of RSP of three-qubit equatorial state with decoherence rate ω and state parameter θ.

3.6. The bit-phase flip noise

Next, we study the influence of bit-phase flip noise on the remote preparation of three-qubit equatorial states. The Kraus operators of this noise can be represented as

$$E_0=\sqrt{1-\gamma}\begin{pmatrix}1&0\\0&1\end{pmatrix},\quad E_1=\sqrt{\gamma}\begin{pmatrix}0&-\mathrm{i}\\\mathrm{i}&0\end{pmatrix}, \tag{29}$$

where γ indicates the decoherence rate. It is observed that the bit-phase flip is the combination of a phase flip and a bit flip. In bit-phase flip noisy transmission environment, the quantum channels between Alice and Bob evolve into

$$\xi_{A_1A_2A_3B_1B_2B_3}(\rho)$$
$$=\frac{1}{8(1-\gamma)^3+8\gamma^3}[(1-\gamma)^3(|000000\rangle+|001001\rangle$$
$$+|010010\rangle+|011011\rangle+|100100\rangle+|101101\rangle$$
$$+|110110\rangle+|111111\rangle)\otimes(\langle 000000|+\langle 001001|$$
$$+\langle 010010|+\langle 011011|+\langle 100100|+\langle 101101|$$
$$+\langle 110110|+\langle 111111|)-\gamma^3(-|111000\rangle+|110001\rangle$$
$$+|101010\rangle-|100011\rangle+|011100\rangle-|010101\rangle$$
$$-|001110\rangle+|000111\rangle)$$
$$\otimes(\langle 111000|-\langle 110001|-\langle 101010|+\langle 100011|$$
$$-\langle 011100|+\langle 010101|+\langle 001110|-\langle 000111|)]. \tag{30}$$

The final state obtained by Bob after the measurement and recovery operations gives

$$\rho_{\mathrm{out}B_1B_2B_3}$$
$$=\frac{1}{8(1-\gamma)^3+8\gamma^3}[(1-\gamma)^3(\mathrm{e}^{\mathrm{i}\theta_0}|000\rangle+\mathrm{e}^{\mathrm{i}\theta_1}|001\rangle$$
$$+\mathrm{e}^{\mathrm{i}\theta_2}|010\rangle+\mathrm{e}^{\mathrm{i}\theta_3}|011\rangle+\mathrm{e}^{\mathrm{i}\theta_4}|100\rangle+\mathrm{e}^{\mathrm{i}\theta_5}|101\rangle$$
$$+\mathrm{e}^{\mathrm{i}\theta_6}|110\rangle+\mathrm{e}^{\mathrm{i}\theta_7}|111\rangle)\otimes(\mathrm{e}^{-\mathrm{i}\theta_0}\langle 000|+\mathrm{e}^{-\mathrm{i}\theta_1}\langle 001|$$
$$+\mathrm{e}^{-\mathrm{i}\theta_2}\langle 010|+\mathrm{e}^{-\mathrm{i}\theta_3}\langle 011|+\mathrm{e}^{-\mathrm{i}\theta_4}\langle 100|+\mathrm{e}^{-\mathrm{i}\theta_5}\langle 101|$$
$$+\mathrm{e}^{-\mathrm{i}\theta_6}\langle 110|+\mathrm{e}^{-\mathrm{i}\theta_7}\langle 111|)-\gamma^3(-\mathrm{e}^{\mathrm{i}\theta_7}|000\rangle+\mathrm{e}^{\mathrm{i}\theta_6}|001\rangle$$
$$+\mathrm{e}^{\mathrm{i}\theta_5}|010\rangle-\mathrm{e}^{\mathrm{i}\theta_4}|011\rangle+\mathrm{e}^{\mathrm{i}\theta_3}|100\rangle-\mathrm{e}^{\mathrm{i}\theta_2}|101\rangle$$
$$-\mathrm{e}^{\mathrm{i}\theta_1}|110\rangle+\mathrm{e}^{\mathrm{i}\theta_0}|111\rangle)\otimes(\mathrm{e}^{-\mathrm{i}\theta_7}\langle 000|-\mathrm{e}^{-\mathrm{i}\theta_6}\langle 001|$$
$$-\mathrm{e}^{-\mathrm{i}\theta_5}\langle 010|+\mathrm{e}^{-\mathrm{i}\theta_4}\langle 011|-\mathrm{e}^{-\mathrm{i}\theta_3}\langle 100|$$
$$+\mathrm{e}^{-\mathrm{i}\theta_2}\langle 101|+\mathrm{e}^{-\mathrm{i}\theta_1}\langle 110|-\mathrm{e}^{-\mathrm{i}\theta_0}\langle 111|)]. \tag{31}$$

We calculate that the fidelity of the final state under the bit-phase flip noise is

$$F=\frac{1}{(1-\gamma)^3+\gamma^3}\left\{(1-\gamma)^3+\frac{1}{16}\gamma^3[\sin(\theta_7-\theta_0)\right.$$
$$\left.-\sin(\theta_6-\theta_1)-\sin(\theta_5-\theta_2)+\sin(\theta_4-\theta_3)]^2\right\}. \tag{32}$$

Obviously, the fidelity of state preparation under bit-phase flip noise is related to both the noise factor and the phase information of the target state. We choose $\theta_7-\theta_0=\theta$, and $\theta_6-\theta_1=\theta_5-\theta_2=\theta_4-\theta_3=0$ for simplicity, to analyze the relationship among fidelity and the noise factor γ and phase factor θ in Fig. 6. Figure 6(a) shows that the fidelity decreases with the increase of γ but will have a slight fluctuation with the change of θ. To exhibit the fluctuation of the fidelity more clearly, we capture a small range illustration for $\gamma\in[0.8,1.0]$, as shown in Fig. 6(b). For a given γ, the fidelity curve has a inflection point and a small peak value at $\theta=\pi/2$. Another thing to note is that if we choose $\theta_7-\theta_0=\theta_6-\theta_1=\theta_5-\theta_2=\theta_4-\theta_3$ as in Subsections 3.2 and 3.5, then the fidelity under bit-phase flip noise is consistent with the fidelity under phase flip noise.

To facilitate the comparison of the influence of different noise channels on the remote preparation of three-qubit equatorial states, the relationship between noise factors and the fidelities of the final states are drawn in Fig. 7 under the same phase parameters. As can be seen, the fidelity changes under bit flip noise, phase damping noise, depolarizing noise, phase flip noise, and bit-phase flip noise tend to be consistent. But when the noise factors equal 1, only the fidelities under bit flip noise, phase flip noise, depolarizing noise, and bit-phase flip noise equal to 0. When the noise factors are in the interval 0–0.4, the fidelities of remote state preparation under the six types of noise can almost be maintained above 0.8. Moreover, the fidelity under depolarizing noise is almost invariably greater than that of other noise for small noise factor (0–0.7), while the fidelity under amplitude damping noise is almost invariably greater than that of other noise for large noise factor (more than 0.7).

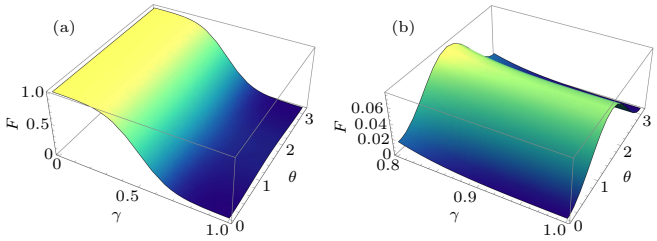


Fig. 6. (a) The fidelity of RSP of three-qubit equatorial state with decoherence rate γ and state parameter θ. (b) The fidelity of RSP with decoherence rate $\gamma \in [0.8, 1.0]$ and θ.

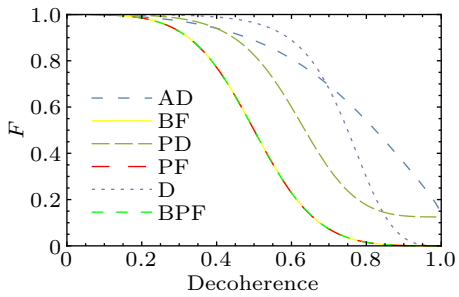


Fig. 7. The contrastive fidelities of RSP of three-qubit equatorial state in amplitude damping (AD) noise, phase damping (PD) noise, bit flip (BF) noise, phase flip (PF) noise, bit-phase flip (BPF) noise, and depolarizing (D) noise with decoherence rate for $\theta_7-\theta_0=\theta_6-\theta_1=\theta_5-\theta_2=\theta_4-\theta_3=\pi/2$.

4. RSP of four-qubit equatorial states in common noisy environments

Next, we explore the RSP of four-qubit equatorial states in six common noisy environments. Here, the target four-qubit equatorial state can be expressed as

$$\begin{aligned}|\chi\rangle = \frac{1}{4}(&e^{i\theta_0}|0000\rangle + e^{i\theta_1}|0001\rangle + e^{i\theta_2}|0010\rangle + e^{i\theta_3}|0011\rangle\\ &+e^{i\theta_4}|0100\rangle + e^{i\theta_5}|0101\rangle + e^{i\theta_6}|0110\rangle + e^{i\theta_7}|0111\rangle\\ &+e^{i\theta_8}|1000\rangle + e^{i\theta_9}|1001\rangle + e^{i\theta_{10}}|1010\rangle + e^{i\theta_{11}}|1011\rangle\\ &+e^{i\theta_{12}}|1100\rangle + e^{i\theta_{13}}|1101\rangle\\ &+e^{i\theta_{14}}|1110\rangle + e^{i\theta_{15}}|1111\rangle). \end{aligned} \tag{33}$$

The quantum channels between Alice and Bob are four two-qubit entangled Bell states

$$\begin{aligned}&|\Psi\rangle_{A_1A_2A_3A_4B_1B_2B_3B_4}\\ &= \frac{1}{4}(|00\rangle_{A_1B_1}+|11\rangle_{A_1B_1})(|00\rangle_{A_2B_2}+|11\rangle_{A_2B_2})(|00\rangle_{A_3B_3}\\ &+|11\rangle_{A_3B_3})(|00\rangle_{A_4B_4}+|11\rangle_{A_4B_4}). \end{aligned} \tag{34}$$

Consider that Bob is the generator of the entangled resource $|\Psi\rangle_{A_1A_2A_3A_4B_1B_2B_3B_4}$. He keeps the particles $\{B_1, B_2, B_3, B_4\}$ and sends the particles $\{A_1, A_2, A_3, A_4\}$ to Alice through the noisy channel. Therefore, in the subsequent RSP process, we only consider the influence of noise on particles $\{A_1, A_2, A_3, A_4\}$. For simplicity, we assume that all particles experience the identical noise.

According to the similar steps in Section 3, we can calculate the prepared final states of the four-qubit equatorial state under the six types of environmental noise, i.e., amplitude damping noise, bit flip noise, phase damping noise, phase flip noise, depolarizing noise, and bit-phase flip noise. The final states of RSP of four-qubit equatorial states in noisy environments are given in the Appendix B. Thus, we can obtain the six fidelities of the final states as follows:

$$\begin{aligned}&F^{AD}\\ &= \frac{[1+4(1-\kappa)^{\frac{1}{2}}+6(1-\kappa)+4(1-\kappa)^{\frac{3}{2}}+(1-\kappa)^2]^2+\kappa^4}{16(16-32\kappa+24\kappa^2-8\kappa^3+2\kappa^4)}, \end{aligned} \tag{35}$$

$$\begin{aligned}F^{BF} = \frac{1}{64(1-\lambda)^4+64\lambda^4}\{&64(1-\lambda)^4+\lambda^4[\cos(\theta_{15}-\theta_0)\\ &+\cos(\theta_{14}-\theta_1)+\cos(\theta_{13}-\theta_2)+\cos(\theta_{12}-\theta_3)\\ &+\cos(\theta_{11}-\theta_4)+\cos(\theta_{10}-\theta_5)+\cos(\theta_9-\theta_6)\\ &+\cos(\theta_8-\theta_7)]^2\}, \end{aligned} \tag{36}$$

$$F^{PD} = \frac{128(1-\mu)^4+\mu^4}{128(1-\mu)^4+16\mu^4}, \tag{37}$$

$$F^{PF} = \frac{(1-\eta)^4}{(1-\eta)^4+\eta^4}, \tag{38}$$

$$\begin{aligned}F^{D} = \frac{1}{64(1-\omega)^4+64(\omega/3)^4}\{&64(1-\omega)^4\\ &+(\omega/3)^4\{[\cos(\theta_{15}-\theta_0)+\cos(\theta_{14}-\theta_1)\\ &+\cos(\theta_{13}-\theta_2)+\cos(\theta_{12}-\theta_3)+\cos(\theta_{11}-\theta_4)\\ &+\cos(\theta_{10}-\theta_5)+\cos(\theta_9-\theta_6)+\cos(\theta_8-\theta_7)]^2\\ &-[\cos(\theta_{15}-\theta_0)-\cos(\theta_{14}-\theta_1)-\cos(\theta_{13}-\theta_2)\\ &+\cos(\theta_{12}-\theta_3)-\cos(\theta_{11}-\theta_4)+\cos(\theta_{10}-\theta_5)\\ &+\cos(\theta_9-\theta_6)-\cos(\theta_8-\theta_7)]^2\}\}, \end{aligned} \tag{39}$$

$$F^{BPF} = \frac{1}{4[16(1-\gamma)^4+16\gamma^4]}\{64(1-\gamma)^4$$

$$+\gamma^4[\cos(\theta_{15}-\theta_0)-\cos(\theta_{14}-\theta_1)-\cos(\theta_{13}-\theta_2)$$
$$+\cos(\theta_{12}-\theta_3)-\cos(\theta_{11}-\theta_4)+\cos(\theta_{10}-\theta_5)$$
$$+\cos(\theta_9-\theta_6)-\cos(\theta_8-\theta_7)]^2\}. \quad (40)$$

Therefore, we can compare the fidelities of the final four-qubit equatorial states under different noisy channels in Fig. 8 under the same phase parameters. As can be seen, the fidelity curves under amplitude damping noise, phase damping noise, bit flip noise, phase flip noise, depolarizing noise, and bit-phase flip noise are similar with the three-qubit equatorial state preparation results in Fig. 7. Compared with the three-qubit scheme, there are just different minimum values for fidelities under amplitude damping noise and phase damping noise. We also plot the fidelity diagrams of RSP of four-qubit equatorial state with decoherence rates and phase parameter θ in bit flip noise and depolarizing noise in Fig. 9. The trends of fidelities are also similar to those in Figs. 2(b) and 5(b).

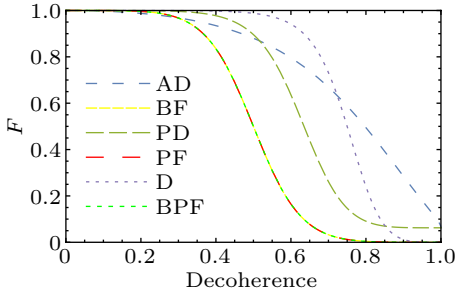


Fig. 8. The contrastive fidelities of RSP of four-qubit equatorial state in amplitude damping noise, phase damping noise, bit flip noise, phase flip noise, bit-phase flip noise, and depolarizing noise with decoherence rate for $\theta_{15}-\theta_0=\theta_{14}-\theta_1=\theta_{13}-\theta_2=\theta_{12}-\theta_3=\theta_{11}-\theta_4=\theta_{10}-\theta_5=\theta_9-\theta_6=\theta_8-\theta_7=\pi/2$.

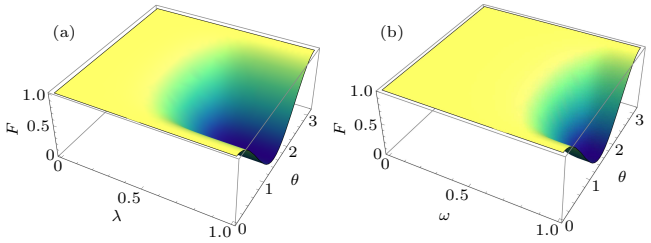


Fig. 9. (a) The fidelity of RSP of four-qubit equatorial state with decoherence rate λ and state parameter θ in bit flip noise. (b) The fidelity of RSP of four-qubit equatorial state with decoherence rate ω and state parameter θ in depolarizing noise. Here, we have taken $\theta_{15}-\theta_0=\theta_{14}-\theta_1=\theta_{13}-\theta_2=\theta_{12}-\theta_3=\theta_{11}-\theta_4=\theta_{10}-\theta_5=\theta_9-\theta_6=\theta_8-\theta_7=\theta$.

5. RSP process in a non-Markov environment

Next, we consider the RSP schemes of multi-qubit equatorial states under the influence of non-Markov environments, which are markedly different from the the previous six noise mechanisms. Due to the memory effect of the non-Markov environment, when an open quantum system evolves in it, part of the information flowing from the system to the environment will flow back from the environment to the system, which oscillates the decoherence process of quantum state.

Similar to the above sections, we consider that only the particles in Alice's hand are affected by non-Markov noise in the remote preparation process of the three-qubit and four-qubit equatorial states, and qubits are resonantly coupled to their own local non-Markov environments. We assume that the environment has a spectral density of the Lorentzian form

$$J(\omega_r)=\frac{1}{2\pi}\frac{\gamma_0\lambda_0^2}{(\omega_r-\omega_0)^2+\lambda_0^2}, \quad (41)$$

where ω_0 is the transition frequency of the qubit, ω_r is the frequency of the environment, γ_0 is the decay rate of the qubit under the Markovian limit, and λ_0 is the spectral width of coupling. Assume that the environment is a zero temperature environment in the vacuum state, then the Kraus operators of the non-Markov effect can be written as[58]

$$E_0(t)=\begin{pmatrix}1 & 0\\ 0 & \sqrt{\mu(t)}\end{pmatrix},\quad E_1(t)=\begin{pmatrix}0 & \sqrt{1-\mu(t)}\\ 0 & 0\end{pmatrix}, \quad (42)$$

where

$$\mu(t)=e^{-\lambda_0 t}\left[\cos\left(\frac{\sqrt{2\lambda_0\gamma_0-\lambda_0^2}t}{2}\right)+\frac{\lambda_0}{\sqrt{2\lambda_0\gamma_0-\lambda_0^2}}\sin\left(\frac{\sqrt{2\lambda_0\gamma_0-\lambda_0^2}t}{2}\right)\right] \quad (43)$$

describes the qubit decay caused by interacting with the non-Markov environment. In such a noisy environment, the dynamics of quantum system can be described as $\rho(t)=\sum_{i=0}^{1}E_i(t)\rho(0)E_i^{\dagger}(t)$.

Hence, the quantum channel between Alice and Bob under the influence of non-Markov noise evolves into

$$\begin{aligned}&\xi_{A_1A_2A_3B_1B_2B_3}(\rho)\\ &=\frac{1}{2+6\mu^2(t)}[(|000000\rangle+\mu^{\frac{1}{2}}(t)|001001\rangle+\mu^{\frac{1}{2}}(t)|010010\rangle\\ &+\mu(t)|011011\rangle+\mu^{\frac{1}{2}}(t)|100100\rangle+\mu(t)|101101\rangle\\ &+\mu(t)|110110\rangle+\mu^{\frac{3}{2}}(t)|111111\rangle)\otimes(\langle 000000|\\ &+\mu^{\frac{1}{2}}(t)\langle 001001|+\mu^{\frac{1}{2}}(t)\langle 010010|+\mu(t)\langle 011011|\\ &+\mu^{\frac{1}{2}}(t)\langle 100100|+\mu(t)\langle 101101|+\mu(t)\langle 110110|\\ &+\mu^{\frac{3}{2}}(t)\langle 111111|)+(1-\mu(t))^3|000111\rangle\langle 000111|]. \quad (44)\end{aligned}$$

The final state after Alice's measurements and Bob's unitary operations becomes

$$\begin{aligned}&\rho_{outB_1B_2B_3}\\ &=\frac{1}{2+6\mu^2(t)}[(e^{i\theta_0}|000\rangle+\mu^{\frac{1}{2}}(t)e^{i\theta_1}|001\rangle+\mu^{\frac{1}{2}}(t)e^{i\theta_2}|010\rangle\\ &+\mu(t)e^{i\theta_3}|011\rangle+\mu^{\frac{1}{2}}(t)e^{i\theta_4}|100\rangle+\mu(t)e^{i\theta_5}|101\rangle\\ &+\mu(t)e^{i\theta_6}|110\rangle+\mu^{\frac{3}{2}}(t)e^{i\theta_7}|111\rangle)\otimes(e^{-i\theta_0}\langle 000|\\ &+\mu^{\frac{1}{2}}(t)e^{-i\theta_1}\langle 001|+\mu^{\frac{1}{2}}(t)e^{-i\theta_2}\langle 010|+\mu(t)e^{-i\theta_3}\langle 011|\end{aligned}$$

$$+\mu^{\frac{1}{2}}(t)\mathrm{e}^{-\mathrm{i}\theta_4}\langle 100|+\mu(t)\mathrm{e}^{-\mathrm{i}\theta_5}\langle 101|+\mu(t)\mathrm{e}^{-\mathrm{i}\theta_6}\langle 110|$$
$$+\mu^{\frac{3}{2}}(t)\mathrm{e}^{-\mathrm{i}\theta_7}\langle 111|)+(1-\mu(t))^3|111\rangle\langle 111|]. \quad (45)$$

And then the fidelity of the final state compared with the ideal state is

$$F = \frac{1}{8(2+6\mu^2(t))}[(1+3\mu^{\frac{1}{2}}(t)+3\mu(t)+\mu^{\frac{3}{2}}(t))^2 +(1-\mu(t))^3]. \quad (46)$$

Figure 10 shows the fidelity diagram of the three-qubit equatorial states in non-Markov environmental noise. As can be seen, there will be an up-and-down oscillation phenomenon with the increase of $\lambda_0 t$. Even for long evolution time, the fidelity gradually approaches 0.1 rather than 0. Damping oscillation is a characteristic of the non-Markov process, which reflects the information flow back and forth between the system and the environment.

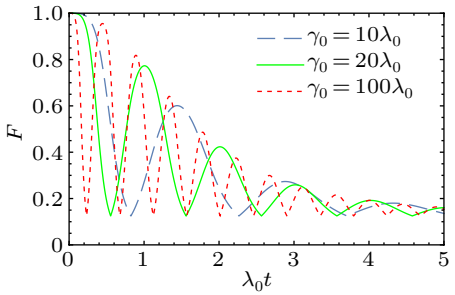


Fig. 10. The fidelity diagram of the three-qubit equatorial states in non-Markov environmental noise with $\gamma_0 = 10\lambda_0$, $\gamma_0 = 20\lambda_0$ and $\gamma_0 = 100\lambda_0$.

For the RSP of four-qubit equatorial states, the effect of non-Markov environmental noise on the process is similar to that of the three-qubit equatorial state. Through direct calculation, the quantum channel of four-qubit scheme under the influence of non-Markov noise gives

$$\xi_{A_1A_2A_3A_4B_1B_2B_3B_4}(\rho)$$
$$= \frac{1}{2+12\mu^2(t)+2\mu^4(t)}[(|00000000\rangle+\mu^{\frac{1}{2}}(t)|00010001\rangle$$
$$+\mu^{\frac{1}{2}}(t)|00100010\rangle+\mu(t)|00110011\rangle+\mu^{\frac{1}{2}}(t)|01000100\rangle$$
$$+\mu(t)|01010101\rangle+\mu(t)|01100110\rangle+\mu^{\frac{3}{2}}(t)|01110111\rangle$$
$$+\mu^{\frac{1}{2}}(t)|10001000\rangle+\mu(t)|10011001\rangle+\mu(t)|10101010\rangle$$
$$+\mu^{\frac{3}{2}}(t)|10111011\rangle+\mu(t)|11001100\rangle+\mu^{\frac{3}{2}}(t)|11011101\rangle$$
$$+\mu^{\frac{3}{2}}(t)|11101110\rangle+\mu^2(t)|11111111\rangle)\otimes(\langle 00000000|$$
$$+\mu^{\frac{1}{2}}(t)\langle 00010001|+\mu^{\frac{1}{2}}(t)\langle 00100010|$$
$$+\mu(t)\langle 00110011|+\mu^{\frac{1}{2}}(t)\langle 01000100|+\mu(t)\langle 01010101|$$
$$+\mu(t)\langle 01100110|+\mu^{\frac{3}{2}}(t)\langle 01110111|+\mu^{\frac{1}{2}}(t)\langle 10001000|$$
$$+\mu(t)\langle 10011001|+\mu(t)\langle 10101010|+\mu^{\frac{3}{2}}(t)\langle 10111011|$$
$$+\mu(t)\langle 11001100|+\mu^{\frac{3}{2}}(t)\langle 11011101|$$
$$+\mu^{\frac{3}{2}}(t)\langle 11101110|+\mu^2(t)\langle 11111111|)$$
$$+(1-\mu(t))^4|00001111\rangle\langle 00001111|]. \quad (47)$$

The density matrix of the final state after Alice's measurements and Bob's unitary operations becomes

$$\rho_{\mathrm{out}B_1B_2B_3B_4}$$
$$= \frac{1}{2+12\mu^2(t)+2\mu^4(t)}[(\mathrm{e}^{\mathrm{i}\theta_0}|0000\rangle+\mu^{\frac{1}{2}}(t)\mathrm{e}^{\mathrm{i}\theta_1}|0001\rangle$$
$$+\mu^{\frac{1}{2}}(t)\mathrm{e}^{\mathrm{i}\theta_2}|0010\rangle+\mu(t)\mathrm{e}^{\mathrm{i}\theta_3}|0011\rangle+\mu^{\frac{1}{2}}(t)\mathrm{e}^{\mathrm{i}\theta_4}|0100\rangle$$
$$+\mu(t)\mathrm{e}^{\mathrm{i}\theta_5}|0101\rangle+\mu(t)\mathrm{e}^{\mathrm{i}\theta_6}|0110\rangle+\mu^{\frac{3}{2}}(t)\mathrm{e}^{\mathrm{i}\theta_7}|0111\rangle$$
$$+\mu^{\frac{1}{2}}(t)\mathrm{e}^{\mathrm{i}\theta_8}|1000\rangle+\mu(t)\mathrm{e}^{\mathrm{i}\theta_9}|1001\rangle+\mu(t)\mathrm{e}^{\mathrm{i}\theta_{10}}|1010\rangle$$
$$+\mu^{\frac{3}{2}}(t)\mathrm{e}^{\mathrm{i}\theta_{11}}|1011\rangle+\mu(t)\mathrm{e}^{\mathrm{i}\theta_{12}}|1100\rangle+\mu^{\frac{3}{2}}(t)\mathrm{e}^{\mathrm{i}\theta_{13}}|1101\rangle$$
$$+\mu^{\frac{3}{2}}(t)\mathrm{e}^{\mathrm{i}\theta_{14}}|1110\rangle+\mu^2(t)\mathrm{e}^{\mathrm{i}\theta_{15}}|1111\rangle)\otimes(\mathrm{e}^{-\mathrm{i}\theta_0}\langle 0000|$$
$$+\mu^{\frac{1}{2}}(t)\mathrm{e}^{-\mathrm{i}\theta_1}\langle 0001|+\mu^{\frac{1}{2}}(t)\mathrm{e}^{-\mathrm{i}\theta_2}\langle 0010|$$
$$+\mu(t)\mathrm{e}^{-\mathrm{i}\theta_3}\langle 0011|+\mu^{\frac{1}{2}}(t)\mathrm{e}^{-\mathrm{i}\theta_4}\langle 0100|+\mu(t)\mathrm{e}^{-\mathrm{i}\theta_5}\langle 0101|$$
$$+\mu(t)\mathrm{e}^{-\mathrm{i}\theta_6}\langle 0110|+\mu^{\frac{3}{2}}(t)\mathrm{e}^{-\mathrm{i}\theta_7}\langle 0111|+\mu^{\frac{1}{2}}(t)\mathrm{e}^{-\mathrm{i}\theta_8}\langle 1000|$$
$$+\mu(t)\mathrm{e}^{-\mathrm{i}\theta_9}\langle 1001|+\mu(t)\mathrm{e}^{-\mathrm{i}\theta_{10}}\langle 1010|+\mu^{\frac{3}{2}}(t)\mathrm{e}^{-\mathrm{i}\theta_{11}}\langle 1011|$$
$$+\mu(t)\mathrm{e}^{-\mathrm{i}\theta_{12}}\langle 1100|+\mu^{\frac{3}{2}}(t)\mathrm{e}^{-\mathrm{i}\theta_{13}}\langle 1101|$$
$$+\mu^{\frac{3}{2}}(t)\mathrm{e}^{-\mathrm{i}\theta_{14}}\langle 1110|+\mu^2(t)\mathrm{e}^{-\mathrm{i}\theta_{15}}\langle 1111|)$$
$$+(1-\mu(t))^4|1111\rangle\langle 1111|]. \quad (48)$$

The fidelity of the final state under the influence of non-Markov environmental noise is

$$F = \frac{1}{32(1+6\mu^2(t)+\mu^4(t))}[(1+4\mu^{\frac{1}{2}}(t)+6\mu(t)+4\mu^{\frac{3}{2}}(t) +\mu^2(t))^2+(1-\mu(t))^4]. \quad (49)$$

Figure 11 shows the fidelity diagram of the four-qubit equatorial states in non-Markov environmental noise with $\lambda_0 t$. As can be seen, the fidelity also shows oscillatory variation. With the increase of t, the fidelity gradually approaches 0.05 after several damping oscillations. Compared to Fig. 10, the fidelity minimum is smaller. This happens because the target state has a higher number of particles and more channel particles are subjected to noise, and the fidelity is affected more.

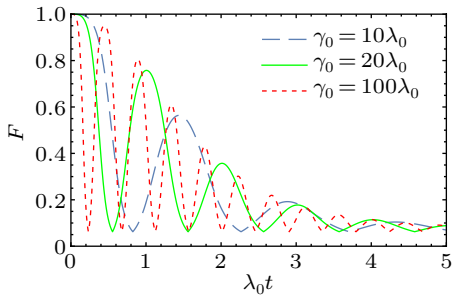


Fig. 11. The fidelity diagram of the four-qubit equatorial states in non-Markov environmental noise with $\gamma_0 = 10\lambda_0$, $\gamma_0 = 20\lambda_0$ and $\gamma_0 = 100\lambda_0$.

6. Discussion and conclusion

RSP schemes are significant for the construction of distributed quantum communication and quantum network. In the actual environment, information will inevitably be affected by different types of environmental noise in the storage and transmission processes. In this paper, by studying the remote preparation of multi-qubit equatorial states in noisy environments, we find that the fidelities of the schemes depend on the decoherence rates of the environmental noises. Generally, the fidelity decreases as the decoherence rate increases. For the six types of common noise, i.e., amplitude damping noise, bit flip noise, phase damping noise, phase flip noise, bit-phase flip noise and depolarizing noise, when the noise factors are equal, the influence of bit flip noise and phase flip noise are similar. When the noise factors are in the small range, the effect of depolarizing noise on RSP is minimal. The information loss caused by amplitude damping noise is less than other noises when the noise factors are large. In particular, when the target state has specific phase information, the bit flip noise and depolarizing noise may have more complex effects on our RSP schemes, even for the ideal cases where the fidelity values are always 1. For the non-Markov environment, owing to the back and forth of information between the environment and systems, fidelities exhibit oscillating behavior and the minimum value may stay greater than zero for a long evolutionary time. These results may have important implications for future research on how to avoid the influence of noise on distributed quantum communication.

Here, our RSP schemes mainly focus on the effects of various types of environmental noise on multi-qubit equatorial states. The results show that noise inevitably reduces the fidelities of the RSP process. In fact, we can design appropriate operations to reduce the negative effects of noises and improve the fidelities of state preparation schemes. For example, it has been proven that weak measurements and quantum reversing measurements of qubits can suppress the influence of environmental noises on quantum states and improve the fidelities of remote preparation of quantum states.[25,29] In our schemes, performing appropriate weak measurements and quantum reversing measurements on transmitted particles in the quantum channel can theoretically improve the fidelities, and the cost of the improved fidelities may be reduced successful probabilities of state preparations. Moreover, the schemes that we considered are remote realization of states preparation by two spatially distant participants. In fact, when it comes to the remote preparation schemes of multi-qubit states, we can theoretically extend the schemes to the controlled RSP schemes or joint RSP schemes. That is, the initial particles can be distributed in the hands of more than one sender or controller. The final success requires the cooperation of multiple senders or controllers. Such schemes are more valuable for the confidentiality of long-distance quantum communication networks.

Appendix A: The explicit derivation procedure from Eq. (10) to Eq. (11)

Under the influence of amplitude damping noise, the quantum channel of participants evolves into the state of Eq. (10). Subsequently, Alice carries out projection measurement of particles in her hand, and the basis vectors of measurement can be expressed as follows:

$$
\begin{aligned}
|\Gamma_1\rangle_{A_1A_2A_3} &= \frac{1}{2\sqrt{2}}(\mathrm{e}^{-\mathrm{i}\theta_0}\langle 000| + \mathrm{e}^{-\mathrm{i}\theta_1}\langle 001| + \mathrm{e}^{-\mathrm{i}\theta_2}\langle 010| \\
&\quad + \mathrm{e}^{-\mathrm{i}\theta_3}\langle 011| + \mathrm{e}^{-\mathrm{i}\theta_4}\langle 100| + \mathrm{e}^{-\mathrm{i}\theta_5}\langle 101| \\
&\quad + \mathrm{e}^{-\mathrm{i}\theta_6}\langle 110| + \mathrm{e}^{-\mathrm{i}\theta_7}\langle 111|), \\
|\Gamma_2\rangle_{A_1A_2A_3} &= \sigma_{A_{1z}} \otimes I_{A_2} \otimes I_{A_3}|\Gamma_1\rangle_{A_1A_2A_3}, \\
|\Gamma_3\rangle_{A_1A_2A_3} &= I_{A_1} \otimes \sigma_{A_{2z}} \otimes I_{A_3}|\Gamma_1\rangle_{A_1A_2A_3}, \\
|\Gamma_4\rangle_{A_1A_2A_3} &= I_{A_1} \otimes I_{A_2} \otimes \sigma_{A_{3z}}|\Gamma_1\rangle_{A_1A_2A_3}, \\
|\Gamma_5\rangle_{A_1A_2A_3} &= \sigma_{A_{1z}} \otimes \sigma_{A_{2z}} \otimes I_{A_3}|\Gamma_1\rangle_{A_1A_2A_3}, \\
|\Gamma_6\rangle_{A_1A_2A_3} &= \sigma_{A_{1z}} \otimes I_{A_2} \otimes \sigma_{A_{3z}}|\Gamma_1\rangle_{A_1A_2A_3}, \\
|\Gamma_7\rangle_{A_1A_2A_3} &= I_{A_1} \otimes \sigma_{A_{2z}} \otimes \sigma_{A_{3z}}|\Gamma_1\rangle_{A_1A_2A_3}, \\
|\Gamma_8\rangle_{A_1A_2A_3} &= \sigma_{A_{1z}} \otimes \sigma_{A_{2z}} \otimes \sigma_{A_{3z}}|\Gamma_1\rangle_{A_1A_2A_3}.
\end{aligned}
$$

According to the eight different measurement results, the particles in Bob's hand collapse into one of the following eight states:

$$
\begin{aligned}
\rho_1 &= \frac{1}{8-12\kappa+6\kappa^2}\{[\mathrm{e}^{\mathrm{i}\theta_0}|000\rangle + (1-\kappa)^{\frac{1}{2}}\mathrm{e}^{\mathrm{i}\theta_1}|001\rangle \\
&\quad + (1-\kappa)^{\frac{1}{2}}\mathrm{e}^{\mathrm{i}\theta_2}|010\rangle + (1-\kappa)\mathrm{e}^{\mathrm{i}\theta_3}|011\rangle \\
&\quad + (1-\kappa)^{\frac{1}{2}}\mathrm{e}^{\mathrm{i}\theta_4}|100\rangle + (1-\kappa)\mathrm{e}^{\mathrm{i}\theta_5}|101\rangle \\
&\quad + (1-\kappa)\mathrm{e}^{\mathrm{i}\theta_6}|110\rangle + (1-\kappa)^{\frac{3}{2}}\mathrm{e}^{\mathrm{i}\theta_7}|111\rangle] \otimes [\mathrm{e}^{-\mathrm{i}\theta_0}\langle 000| \\
&\quad + (1-\kappa)^{\frac{1}{2}}\mathrm{e}^{-\mathrm{i}\theta_1}\langle 001| + (1-\kappa)^{\frac{1}{2}}\mathrm{e}^{-\mathrm{i}\theta_2}\langle 010| \\
&\quad + (1-\kappa)\mathrm{e}^{-\mathrm{i}\theta_3}\langle 011| + (1-\kappa)^{\frac{1}{2}}\mathrm{e}^{-\mathrm{i}\theta_4}\langle 100| \\
&\quad + (1-\kappa)\mathrm{e}^{-\mathrm{i}\theta_5}\langle 101| + (1-\kappa)\mathrm{e}^{-\mathrm{i}\theta_6}\langle 110| \\
&\quad + (1-\kappa)^{\frac{3}{2}}\mathrm{e}^{-\mathrm{i}\theta_7}\langle 111|] + \kappa^3|111\rangle\langle 111|\}, \\
\rho_2 &= \frac{1}{8-12\kappa+6\kappa^2}\{[\mathrm{e}^{\mathrm{i}\theta_0}|000\rangle + (1-\kappa)^{\frac{1}{2}}\mathrm{e}^{\mathrm{i}\theta_1}|001\rangle \\
&\quad + (1-\kappa)^{\frac{1}{2}}\mathrm{e}^{\mathrm{i}\theta_2}|010\rangle + (1-\kappa)\mathrm{e}^{\mathrm{i}\theta_3}|011\rangle \\
&\quad - (1-\kappa)^{\frac{1}{2}}\mathrm{e}^{\mathrm{i}\theta_4}|100\rangle - (1-\kappa)\mathrm{e}^{\mathrm{i}\theta_5}|101\rangle \\
&\quad - (1-\kappa)\mathrm{e}^{\mathrm{i}\theta_6}|110\rangle - (1-\kappa)^{\frac{3}{2}}\mathrm{e}^{\mathrm{i}\theta_7}|111\rangle] \otimes [\mathrm{e}^{-\mathrm{i}\theta_0}\langle 000| \\
&\quad + (1-\kappa)^{\frac{1}{2}}\mathrm{e}^{-\mathrm{i}\theta_1}\langle 001| + (1-\kappa)^{\frac{1}{2}}\mathrm{e}^{-\mathrm{i}\theta_2}\langle 010| \\
&\quad + (1-\kappa)\mathrm{e}^{-\mathrm{i}\theta_3}\langle 011| - (1-\kappa)^{\frac{1}{2}}\mathrm{e}^{-\mathrm{i}\theta_4}\langle 100| \\
&\quad - (1-\kappa)\mathrm{e}^{-\mathrm{i}\theta_5}\langle 101| - (1-\kappa)\mathrm{e}^{-\mathrm{i}\theta_6}\langle 110|
\end{aligned}
$$

$$
\begin{aligned}
&-(1-\kappa)^{\frac{3}{2}}\mathrm{e}^{-\mathrm{i}\theta_7}\langle 111|]+\kappa^3|111\rangle\langle 111|\},\\
\rho_3 = &\frac{1}{8-12\kappa+6\kappa^2}\{[\mathrm{e}^{\mathrm{i}\theta_0}|000\rangle+(1-\kappa)^{\frac{1}{2}}\mathrm{e}^{\mathrm{i}\theta_1}|001\rangle\\
&-(1-\kappa)^{\frac{1}{2}}\mathrm{e}^{\mathrm{i}\theta_2}|010\rangle-(1-\kappa)\mathrm{e}^{\mathrm{i}\theta_3}|011\rangle\\
&+(1-\kappa)^{\frac{1}{2}}\mathrm{e}^{\mathrm{i}\theta_4}|100\rangle+(1-\kappa)\mathrm{e}^{\mathrm{i}\theta_5}|101\rangle\\
&-(1-\kappa)\mathrm{e}^{\mathrm{i}\theta_6}|110\rangle-(1-\kappa)^{\frac{3}{2}}\mathrm{e}^{\mathrm{i}\theta_7}|111\rangle]\otimes[\mathrm{e}^{-\mathrm{i}\theta_0}\langle 000|\\
&+(1-\kappa)^{\frac{1}{2}}\mathrm{e}^{-\mathrm{i}\theta_1}\langle 001|-(1-\kappa)^{\frac{1}{2}}\mathrm{e}^{-\mathrm{i}\theta_2}\langle 010|\\
&-(1-\kappa)\mathrm{e}^{-\mathrm{i}\theta_3}\langle 011|+(1-\kappa)^{\frac{1}{2}}\mathrm{e}^{-\mathrm{i}\theta_4}\langle 100|\\
&+(1-\kappa)\mathrm{e}^{-\mathrm{i}\theta_5}\langle 101|-(1-\kappa)\mathrm{e}^{-\mathrm{i}\theta_6}\langle 110|\\
&-(1-\kappa)^{\frac{3}{2}}\mathrm{e}^{-\mathrm{i}\theta_7}\langle 111|]+\kappa^3|111\rangle\langle 111|\},\\
\rho_4 = &\frac{1}{8-12\kappa+6\kappa^2}\{[\mathrm{e}^{\mathrm{i}\theta_0}|000\rangle-(1-\kappa)^{\frac{1}{2}}\mathrm{e}^{\mathrm{i}\theta_1}|001\rangle\\
&+(1-\kappa)^{\frac{1}{2}}\mathrm{e}^{\mathrm{i}\theta_2}|010\rangle-(1-\kappa)\mathrm{e}^{\mathrm{i}\theta_3}|011\rangle\\
&+(1-\kappa)^{\frac{1}{2}}\mathrm{e}^{\mathrm{i}\theta_4}|100\rangle-(1-\kappa)\mathrm{e}^{\mathrm{i}\theta_5}|101\rangle\\
&+(1-\kappa)\mathrm{e}^{\mathrm{i}\theta_6}|110\rangle-(1-\kappa)^{\frac{3}{2}}\mathrm{e}^{\mathrm{i}\theta_7}|111\rangle]\otimes[\mathrm{e}^{-\mathrm{i}\theta_0}\langle 000|\\
&-(1-\kappa)^{\frac{1}{2}}\mathrm{e}^{-\mathrm{i}\theta_1}\langle 001|+(1-\kappa)^{\frac{1}{2}}\mathrm{e}^{-\mathrm{i}\theta_2}\langle 010|\\
&-(1-\kappa)\mathrm{e}^{-\mathrm{i}\theta_3}\langle 011|+(1-\kappa)^{\frac{1}{2}}\mathrm{e}^{-\mathrm{i}\theta_4}\langle 100|\\
&-(1-\kappa)\mathrm{e}^{-\mathrm{i}\theta_5}\langle 101|+(1-\kappa)\mathrm{e}^{-\mathrm{i}\theta_6}\langle 110|\\
&-(1-\kappa)^{\frac{3}{2}}\mathrm{e}^{-\mathrm{i}\theta_7}\langle 111|]+\kappa^3|111\rangle\langle 111|\},\\
\rho_5 = &\frac{1}{8-12\kappa+6\kappa^2}\{[\mathrm{e}^{\mathrm{i}\theta_0}|000\rangle+(1-\kappa)^{\frac{1}{2}}\mathrm{e}^{\mathrm{i}\theta_1}|001\rangle\\
&-(1-\kappa)^{\frac{1}{2}}\mathrm{e}^{\mathrm{i}\theta_2}|010\rangle-(1-\kappa)\mathrm{e}^{\mathrm{i}\theta_3}|011\rangle\\
&-(1-\kappa)^{\frac{1}{2}}\mathrm{e}^{\mathrm{i}\theta_4}|100\rangle-(1-\kappa)\mathrm{e}^{\mathrm{i}\theta_5}|101\rangle\\
&+(1-\kappa)\mathrm{e}^{\mathrm{i}\theta_6}|110\rangle+(1-\kappa)^{\frac{3}{2}}\mathrm{e}^{\mathrm{i}\theta_7}|111\rangle]\otimes[\mathrm{e}^{-\mathrm{i}\theta_0}\langle 000|\\
&+(1-\kappa)^{\frac{1}{2}}\mathrm{e}^{-\mathrm{i}\theta_1}\langle 001|-(1-\kappa)^{\frac{1}{2}}\mathrm{e}^{-\mathrm{i}\theta_2}\langle 010|\\
&-(1-\kappa)\mathrm{e}^{-\mathrm{i}\theta_3}\langle 011|-(1-\kappa)^{\frac{1}{2}}\mathrm{e}^{-\mathrm{i}\theta_4}\langle 100|\\
&-(1-\kappa)\mathrm{e}^{-\mathrm{i}\theta_5}\langle 101|+(1-\kappa)\mathrm{e}^{-\mathrm{i}\theta_6}\langle 110|\\
&+(1-\kappa)^{\frac{3}{2}}\mathrm{e}^{-\mathrm{i}\theta_7}\langle 111|]+\kappa^3|111\rangle\langle 111|\},\\
\rho_6 = &\frac{1}{8-12\kappa+6\kappa^2}\{[\mathrm{e}^{\mathrm{i}\theta_0}|000\rangle-(1-\kappa)^{\frac{1}{2}}\mathrm{e}^{\mathrm{i}\theta_1}|001\rangle\\
&+(1-\kappa)^{\frac{1}{2}}\mathrm{e}^{\mathrm{i}\theta_2}|010\rangle-(1-\kappa)\mathrm{e}^{\mathrm{i}\theta_3}|011\rangle\\
&-(1-\kappa)^{\frac{1}{2}}\mathrm{e}^{\mathrm{i}\theta_4}|100\rangle+(1-\kappa)\mathrm{e}^{\mathrm{i}\theta_5}|101\rangle\\
&-(1-\kappa)\mathrm{e}^{\mathrm{i}\theta_6}|110\rangle+(1-\kappa)^{\frac{3}{2}}\mathrm{e}^{\mathrm{i}\theta_7}|111\rangle]\otimes[\mathrm{e}^{-\mathrm{i}\theta_0}\langle 000|\\
&-(1-\kappa)^{\frac{1}{2}}\mathrm{e}^{-\mathrm{i}\theta_1}\langle 001|+(1-\kappa)^{\frac{1}{2}}\mathrm{e}^{-\mathrm{i}\theta_2}\langle 010|\\
&-(1-\kappa)\mathrm{e}^{-\mathrm{i}\theta_3}\langle 011|-(1-\kappa)^{\frac{1}{2}}\mathrm{e}^{-\mathrm{i}\theta_4}\langle 100|\\
&+(1-\kappa)\mathrm{e}^{-\mathrm{i}\theta_5}\langle 101|-(1-\kappa)\mathrm{e}^{-\mathrm{i}\theta_6}\langle 110|\\
&+(1-\kappa)^{\frac{3}{2}}\mathrm{e}^{-\mathrm{i}\theta_7}\langle 111|]+\kappa^3|111\rangle\langle 111|\},\\
\rho_7 = &\frac{1}{8-12\kappa+6\kappa^2}\{[\mathrm{e}^{\mathrm{i}\theta_0}|000\rangle-(1-\kappa)^{\frac{1}{2}}\mathrm{e}^{\mathrm{i}\theta_1}|001\rangle\\
&-(1-\kappa)^{\frac{1}{2}}\mathrm{e}^{\mathrm{i}\theta_2}|010\rangle+(1-\kappa)\mathrm{e}^{\mathrm{i}\theta_3}|011\rangle\\
&+(1-\kappa)^{\frac{1}{2}}\mathrm{e}^{\mathrm{i}\theta_4}|100\rangle-(1-\kappa)\mathrm{e}^{\mathrm{i}\theta_5}|101\rangle\\
&-(1-\kappa)\mathrm{e}^{\mathrm{i}\theta_6}|110\rangle+(1-\kappa)^{\frac{3}{2}}\mathrm{e}^{\mathrm{i}\theta_7}|111\rangle]\otimes[\mathrm{e}^{-\mathrm{i}\theta_0}\langle 000|\\
&-(1-\kappa)^{\frac{1}{2}}\mathrm{e}^{-\mathrm{i}\theta_1}\langle 001|-(1-\kappa)^{\frac{1}{2}}\mathrm{e}^{-\mathrm{i}\theta_2}\langle 010|\\
&+(1-\kappa)\mathrm{e}^{-\mathrm{i}\theta_3}\langle 011|+(1-\kappa)^{\frac{1}{2}}\mathrm{e}^{-\mathrm{i}\theta_4}\langle 100|\\
&-(1-\kappa)\mathrm{e}^{-\mathrm{i}\theta_5}\langle 101|-(1-\kappa)\mathrm{e}^{-\mathrm{i}\theta_6}\langle 110|\\
&+(1-\kappa)^{\frac{3}{2}}\mathrm{e}^{-\mathrm{i}\theta_7}\langle 111|]+\kappa^3|111\rangle\langle 111|\},\\
\rho_8 = &\frac{1}{8-12\kappa+6\kappa^2}\{[\mathrm{e}^{\mathrm{i}\theta_0}|000\rangle-(1-\kappa)^{\frac{1}{2}}\mathrm{e}^{\mathrm{i}\theta_1}|001\rangle\\
&-(1-\kappa)^{\frac{1}{2}}\mathrm{e}^{\mathrm{i}\theta_2}|010\rangle+(1-\kappa)\mathrm{e}^{\mathrm{i}\theta_3}|011\rangle\\
&-(1-\kappa)^{\frac{1}{2}}\mathrm{e}^{\mathrm{i}\theta_4}|100\rangle+(1-\kappa)\mathrm{e}^{\mathrm{i}\theta_5}|101\rangle\\
&+(1-\kappa)\mathrm{e}^{\mathrm{i}\theta_6}|110\rangle-(1-\kappa)^{\frac{3}{2}}\mathrm{e}^{\mathrm{i}\theta_7}|111\rangle]\otimes[\mathrm{e}^{-\mathrm{i}\theta_0}\langle 000|\\
&-(1-\kappa)^{\frac{1}{2}}\mathrm{e}^{-\mathrm{i}\theta_1}\langle 001|-(1-\kappa)^{\frac{1}{2}}\mathrm{e}^{-\mathrm{i}\theta_2}\langle 010|\\
&+(1-\kappa)\mathrm{e}^{-\mathrm{i}\theta_3}\langle 011|-(1-\kappa)^{\frac{1}{2}}\mathrm{e}^{-\mathrm{i}\theta_4}\langle 100|\\
&+(1-\kappa)\mathrm{e}^{-\mathrm{i}\theta_5}\langle 101|+(1-\kappa)\mathrm{e}^{-\mathrm{i}\theta_6}\langle 110|\\
&-(1-\kappa)^{\frac{3}{2}}\mathrm{e}^{-\mathrm{i}\theta_7}\langle 111|]+\kappa^3|111\rangle\langle 111|\}.
\end{aligned}
$$

From this, it can be seen that if Bob performs a set of corresponding unitary operations $I_{\mathrm{B}_1}\otimes I_{\mathrm{B}_2}\otimes I_{\mathrm{B}_3}$, $\sigma_{\mathrm{B}_{1z}}\otimes I_{\mathrm{B}_2}\otimes I_{\mathrm{B}_3}$, $I_{\mathrm{B}_1}\otimes\sigma_{\mathrm{B}_{2z}}\otimes I_{\mathrm{B}_3}$, $I_{\mathrm{B}_1}\otimes I_{\mathrm{B}_2}\otimes\sigma_{\mathrm{B}_{3z}}$, $\sigma_{\mathrm{B}_{1z}}\otimes\sigma_{\mathrm{B}_{2z}}\otimes I_{\mathrm{B}_3}$, $\sigma_{\mathrm{B}_{1z}}\otimes I_{\mathrm{B}_2}\otimes\sigma_{\mathrm{B}_{3z}}$, $I_{\mathrm{B}_1}\otimes\sigma_{\mathrm{B}_{2z}}\otimes\sigma_{\mathrm{B}_{3z}}$ or $\sigma_{\mathrm{B}_{1z}}\otimes\sigma_{\mathrm{B}_{2z}}\otimes\sigma_{\mathrm{B}_{3z}}$ on the particles in his hand, then the final state can be obtained as Eq. (11).

For the other noisy environments, the measurement and recovery processes of multi-qubit equatorial state RSP are similar. The tedious derivations of the expressions are not shown here.

Appendix B: The final states of RSP of four-qubit equatorial states in a noisy environment

According to the Kraus operators of six types of noise in Eqs. (9), (13), (17), (21), (25), and (29), we can work out the density matrices of the four-qubit final states obtained by Bob after Alice's projection measurements, respectively.

(i) The final state under amplitude damping noise

$$
\begin{aligned}
\rho_{\mathrm{outB_1B_2B_3B_4}} = &\frac{1}{16-32\kappa+24\kappa^2-8\kappa^3+2\kappa^4}\{[\mathrm{e}^{\mathrm{i}\theta_0}|0000\rangle\\
&+(1-\kappa)^{\frac{1}{2}}\mathrm{e}^{\mathrm{i}\theta_1}|0001\rangle+(1-\kappa)^{\frac{1}{2}}\mathrm{e}^{\mathrm{i}\theta_2}|0010\rangle+(1-\kappa)\mathrm{e}^{\mathrm{i}\theta_3}|0011\rangle\\
&+(1-\kappa)^{\frac{1}{2}}\mathrm{e}^{\mathrm{i}\theta_4}|0100\rangle+(1-\kappa)\mathrm{e}^{\mathrm{i}\theta_5}|0101\rangle+(1-\kappa)\mathrm{e}^{\mathrm{i}\theta_6}|0110\rangle
\end{aligned}
$$

$$
\begin{aligned}
&+(1-\kappa)^{\frac{3}{2}}\mathrm{e}^{\mathrm{i}\theta_7}|0111\rangle+(1-\kappa)^{\frac{1}{2}}\mathrm{e}^{\mathrm{i}\theta_8}|1000\rangle+(1-\kappa)\mathrm{e}^{\mathrm{i}\theta_9}|1001\rangle\\
&+(1-\kappa)\mathrm{e}^{\mathrm{i}\theta_{10}}|1010\rangle+(1-\kappa)^{\frac{3}{2}}\mathrm{e}^{\mathrm{i}\theta_{11}}|1011\rangle+(1-\kappa)\mathrm{e}^{\mathrm{i}\theta_{12}}|1100\rangle\\
&+(1-\kappa)^{\frac{3}{2}}\mathrm{e}^{\mathrm{i}\theta_{13}}|1101\rangle+(1-\kappa)^{\frac{3}{2}}\mathrm{e}^{\mathrm{i}\theta_{14}}|1110\rangle+(1-\kappa)^2\mathrm{e}^{\mathrm{i}\theta_{15}}|1111\rangle]\\
&\otimes[\mathrm{e}^{-\mathrm{i}\theta_0}\langle 0000|+(1-\kappa)^{\frac{1}{2}}\mathrm{e}^{-\mathrm{i}\theta_1}\langle 0001|+(1-\kappa)^{\frac{1}{2}}\mathrm{e}^{-\mathrm{i}\theta_2}\langle 0010|\\
&+(1-\kappa)\mathrm{e}^{-\mathrm{i}\theta_3}\langle 0011|+(1-\kappa)^{\frac{1}{2}}\mathrm{e}^{-\mathrm{i}\theta_4}\langle 0100|+(1-\kappa)\mathrm{e}^{-\mathrm{i}\theta_5}\langle 0101|\\
&+(1-\kappa)\mathrm{e}^{-\mathrm{i}\theta_6}\langle 0110|+(1-\kappa)^{\frac{3}{2}}\mathrm{e}^{-\mathrm{i}\theta_7}\langle 0111|+(1-\kappa)^{\frac{1}{2}}\mathrm{e}^{-\mathrm{i}\theta_8}\langle 1000|\\
&+(1-\kappa)\mathrm{e}^{-\mathrm{i}\theta_9}\langle 1001|+(1-\kappa)\mathrm{e}^{-\mathrm{i}\theta_{10}}\langle 1010|+(1-\kappa)^{\frac{3}{2}}\mathrm{e}^{-\mathrm{i}\theta_{11}}\langle 1011|\\
&+(1-\kappa)\mathrm{e}^{-\mathrm{i}\theta_{12}}\langle 1100|+(1-\kappa)^{\frac{3}{2}}\mathrm{e}^{-\mathrm{i}\theta_{13}}\langle 1101|+(1-\kappa)^{\frac{3}{2}}\mathrm{e}^{-\mathrm{i}\theta_{14}}\langle 1110|\\
&+(1-\kappa)^2\mathrm{e}^{-\mathrm{i}\theta_{15}}\langle 0111|]+\kappa^4|1111\rangle\langle 0111|\}.
\end{aligned}
$$

(ii) The final state under bit flip noise

$$
\begin{aligned}
\rho_{\mathrm{outB_1B_2B_3B_4}} = \frac{1}{16(1-\lambda)^4+16\lambda^4}&[(1-\lambda)^2(\mathrm{e}^{\mathrm{i}\theta_0}|0000\rangle+\mathrm{e}^{\mathrm{i}\theta_1}|0001\rangle+\mathrm{e}^{\mathrm{i}\theta_2}|0010\rangle\\
&+\mathrm{e}^{\mathrm{i}\theta_3}|0011\rangle+\mathrm{e}^{\mathrm{i}\theta_4}|0100\rangle+\mathrm{e}^{\mathrm{i}\theta_5}|0101\rangle+\mathrm{e}^{\mathrm{i}\theta_6}|0110\rangle+\mathrm{e}^{\mathrm{i}\theta_7}|0111\rangle\\
&+\mathrm{e}^{\mathrm{i}\theta_8}|1000\rangle+\mathrm{e}^{\mathrm{i}\theta_9}|1001\rangle+\mathrm{e}^{\mathrm{i}\theta_{10}}|1010\rangle+\mathrm{e}^{\mathrm{i}\theta_{11}}|1011\rangle\\
&+\mathrm{e}^{\mathrm{i}\theta_{12}}|1100\rangle+\mathrm{e}^{\mathrm{i}\theta_{13}}|1101\rangle+\mathrm{e}^{\mathrm{i}\theta_{14}}|1110\rangle+\mathrm{e}^{\mathrm{i}\theta_{15}}|1111\rangle)\\
&\otimes(1-\lambda)^2(\mathrm{e}^{-\mathrm{i}\theta_0}\langle 0000|+\mathrm{e}^{-\mathrm{i}\theta_1}\langle 0001|+\mathrm{e}^{-\mathrm{i}\theta_2}\langle 0010|+\mathrm{e}^{-\mathrm{i}\theta_3}\langle 011|\\
&+\mathrm{e}^{-\mathrm{i}\theta_4}\langle 0100|+\mathrm{e}^{-\mathrm{i}\theta_5}\langle 0101|+\mathrm{e}^{-\mathrm{i}\theta_6}\langle 0110|+\mathrm{e}^{-\mathrm{i}\theta_7}\langle 0111|\\
&+\mathrm{e}^{-\mathrm{i}\theta_8}\langle 1000|+\mathrm{e}^{-\mathrm{i}\theta_9}\langle 1001|+\mathrm{e}^{-\mathrm{i}\theta_{10}}\langle 1010|+\mathrm{e}^{-\mathrm{i}\theta_{11}}\langle 1011|\\
&+\mathrm{e}^{-\mathrm{i}\theta_{12}}\langle 1100|+\mathrm{e}^{-\mathrm{i}\theta_{13}}\langle 1101|+\mathrm{e}^{-\mathrm{i}\theta_{14}}\langle 1110|+\mathrm{e}^{-\mathrm{i}\theta_{15}}\langle 1111|)\\
&+\lambda^2(\mathrm{e}^{\mathrm{i}\theta_{15}}|0000\rangle+\mathrm{e}^{\mathrm{i}\theta_{14}}|0001\rangle+\mathrm{e}^{\mathrm{i}\theta_{13}}|0010\rangle+\mathrm{e}^{\mathrm{i}\theta_{12}}|0011\rangle\\
&+\mathrm{e}^{\mathrm{i}\theta_{11}}|0100\rangle+\mathrm{e}^{\mathrm{i}\theta_{10}}|0101\rangle+\mathrm{e}^{\mathrm{i}\theta_9}|0110\rangle+\mathrm{e}^{\mathrm{i}\theta_8}|0111\rangle\\
&+\mathrm{e}^{\mathrm{i}\theta_7}|1000\rangle+\mathrm{e}^{\mathrm{i}\theta_6}|1001\rangle+\mathrm{e}^{\mathrm{i}\theta_5}|1010\rangle+\mathrm{e}^{\mathrm{i}\theta_4}|1011\rangle\\
&+\mathrm{e}^{\mathrm{i}\theta_3}|1100\rangle+\mathrm{e}^{\mathrm{i}\theta_2}|1101\rangle+\mathrm{e}^{\mathrm{i}\theta_1}|1110\rangle+\mathrm{e}^{\mathrm{i}\theta_0}|1111\rangle)\\
&\otimes\lambda^2(\mathrm{e}^{-\mathrm{i}\theta_{15}}\langle 0000|+\mathrm{e}^{-\mathrm{i}\theta_{14}}\langle 0001|+\mathrm{e}^{-\mathrm{i}\theta_{13}}\langle 0010|+\mathrm{e}^{-\mathrm{i}\theta_{12}}\langle 0011|\\
&+\mathrm{e}^{-\mathrm{i}\theta_{11}}\langle 0100|+\mathrm{e}^{-\mathrm{i}\theta_{10}}\langle 0101|+\mathrm{e}^{-\mathrm{i}\theta_9}\langle 0110|+\mathrm{e}^{-\mathrm{i}\theta_8}\langle 0111|\\
&+\mathrm{e}^{-\mathrm{i}\theta_7}\langle 1000|+\mathrm{e}^{-\mathrm{i}\theta_6}\langle 1001|+\mathrm{e}^{-\mathrm{i}\theta_5}\langle 1010|+\mathrm{e}^{-\mathrm{i}\theta_4}\langle 1011|\\
&+\mathrm{e}^{-\mathrm{i}\theta_3}\langle 1100|+\mathrm{e}^{-\mathrm{i}\theta_2}\langle 1101|+\mathrm{e}^{-\mathrm{i}\theta_1}\langle 1110|+\mathrm{e}^{-\mathrm{i}\theta_0}\langle 1111|)].
\end{aligned}
$$

(iii) The final state under phase damping noise

$$
\begin{aligned}
\rho_{\mathrm{outB_1B_2B_3B_4}} = \frac{1}{16(1-\mu)^4+2\mu^4}&[(1-\mu)^2(\mathrm{e}^{\mathrm{i}\theta_0}|0000\rangle+\mathrm{e}^{\mathrm{i}\theta_1}|0001\rangle+\mathrm{e}^{\mathrm{i}\theta_2}|0010\rangle\\
&+\mathrm{e}^{\mathrm{i}\theta_3}|0011\rangle+\mathrm{e}^{\mathrm{i}\theta_4}|0100\rangle+\mathrm{e}^{\mathrm{i}\theta_5}|0101\rangle+\mathrm{e}^{\mathrm{i}\theta_6}|0110\rangle+\mathrm{e}^{\mathrm{i}\theta_7}|0111\rangle\\
&+\mathrm{e}^{\mathrm{i}\theta_8}|1000\rangle+\mathrm{e}^{\mathrm{i}\theta_9}|1001\rangle+\mathrm{e}^{\mathrm{i}\theta_{10}}|1010\rangle+\mathrm{e}^{\mathrm{i}\theta_{11}}|1011\rangle\\
&+\mathrm{e}^{\mathrm{i}\theta_{12}}|1100\rangle+\mathrm{e}^{\mathrm{i}\theta_{13}}|1101\rangle+\mathrm{e}^{\mathrm{i}\theta_{14}}|1110\rangle+\mathrm{e}^{\mathrm{i}\theta_{15}}|1111\rangle)\\
&\otimes(1-\mu)^2(\mathrm{e}^{-\mathrm{i}\theta_0}\langle 0000|+\mathrm{e}^{-\mathrm{i}\theta_1}\langle 0001|+\mathrm{e}^{-\mathrm{i}\theta_2}\langle 0010|+\mathrm{e}^{-\mathrm{i}\theta_3}\langle 0011|\\
&+\mathrm{e}^{-\mathrm{i}\theta_4}\langle 0100|+\mathrm{e}^{-\mathrm{i}\theta_5}\langle 0101|+\mathrm{e}^{-\mathrm{i}\theta_6}\langle 0110|+\mathrm{e}^{-\mathrm{i}\theta_7}\langle 0111|\\
&+\mathrm{e}^{-\mathrm{i}\theta_8}\langle 1000|+\mathrm{e}^{-\mathrm{i}\theta_9}\langle 1001|+\mathrm{e}^{-\mathrm{i}\theta_{10}}\langle 1010|+\mathrm{e}^{-\mathrm{i}\theta_{11}}\langle 1011|\\
&+\mathrm{e}^{-\mathrm{i}\theta_{12}}\langle 1100|+\mathrm{e}^{-\mathrm{i}\theta_{13}}\langle 1101|+\mathrm{e}^{-\mathrm{i}\theta_{14}}\langle 1110|+\mathrm{e}^{-\mathrm{i}\theta_{15}}\langle 1111|)\\
&+\mu^4|0000\rangle\langle 0000|+\mu^4|1111\rangle\langle 1111|].
\end{aligned}
$$

(iv) The final state under phase flip noise

$$\begin{aligned}\rho_{\mathrm{outB_1B_2B_3B_4}} = \frac{1}{16(1-\eta)^4+16\eta^4}[&(1-\eta)^2(\mathrm{e}^{\mathrm{i}\theta_0}|0000\rangle+\mathrm{e}^{\mathrm{i}\theta_1}|0001\rangle+\mathrm{e}^{\mathrm{i}\theta_2}|0010\rangle\\&+\mathrm{e}^{\mathrm{i}\theta_3}|0011\rangle+\mathrm{e}^{\mathrm{i}\theta_4}|0100\rangle+\mathrm{e}^{\mathrm{i}\theta_5}|0101\rangle+\mathrm{e}^{\mathrm{i}\theta_6}|0110\rangle+\mathrm{e}^{\mathrm{i}\theta_7}|0111\rangle\\&+\mathrm{e}^{\mathrm{i}\theta_8}|1000\rangle+\mathrm{e}^{\mathrm{i}\theta_9}|1001\rangle+\mathrm{e}^{\mathrm{i}\theta_{10}}|1010\rangle+\mathrm{e}^{\mathrm{i}\theta_{11}}|1011\rangle\\&+\mathrm{e}^{\mathrm{i}\theta_{12}}|1100\rangle+\mathrm{e}^{\mathrm{i}\theta_{13}}|1101\rangle+\mathrm{e}^{\mathrm{i}\theta_{14}}|1110\rangle+\mathrm{e}^{\mathrm{i}\theta_{15}}|1111\rangle)\\&\otimes(1-\eta)^2(\mathrm{e}^{-\mathrm{i}\theta_0}\langle0000|+\mathrm{e}^{-\mathrm{i}\theta_1}\langle0001|+\mathrm{e}^{-\mathrm{i}\theta_2}\langle0010|+\mathrm{e}^{-\mathrm{i}\theta_3}\langle0011|\\&+\mathrm{e}^{-\mathrm{i}\theta_4}\langle0100|+\mathrm{e}^{-\mathrm{i}\theta_5}\langle0101|+\mathrm{e}^{-\mathrm{i}\theta_6}\langle0110|+\mathrm{e}^{-\mathrm{i}\theta_7}\langle0111|\\&+\mathrm{e}^{-\mathrm{i}\theta_8}\langle1000|+\mathrm{e}^{-\mathrm{i}\theta_9}\langle1001|+\mathrm{e}^{-\mathrm{i}\theta_{10}}\langle1010|+\mathrm{e}^{-\mathrm{i}\theta_{11}}\langle1011|\\&+\mathrm{e}^{-\mathrm{i}\theta_{12}}\langle1100|+\mathrm{e}^{-\mathrm{i}\theta_{13}}\langle1101|+\mathrm{e}^{-\mathrm{i}\theta_{14}}\langle1110|+\mathrm{e}^{-\mathrm{i}\theta_{15}}\langle1111|)\\&+\eta^2(\mathrm{e}^{\mathrm{i}\theta_0}|0000\rangle-\mathrm{e}^{\mathrm{i}\theta_1}|0001\rangle-\mathrm{e}^{\mathrm{i}\theta_2}|0010\rangle+\mathrm{e}^{\mathrm{i}\theta_3}|0011\rangle\\&-\mathrm{e}^{\mathrm{i}\theta_4}|0100\rangle+\mathrm{e}^{\mathrm{i}\theta_5}|0101\rangle+\mathrm{e}^{\mathrm{i}\theta_6}|0110\rangle-\mathrm{e}^{\mathrm{i}\theta_7}|0111\rangle\\&-\mathrm{e}^{\mathrm{i}\theta_8}|1000\rangle+\mathrm{e}^{\mathrm{i}\theta_9}|1001\rangle+\mathrm{e}^{\mathrm{i}\theta_{10}}|1010\rangle-\mathrm{e}^{\mathrm{i}\theta_{11}}|1011\rangle\\&+\mathrm{e}^{\mathrm{i}\theta_{12}}|1100\rangle-\mathrm{e}^{\mathrm{i}\theta_{13}}|1101\rangle-\mathrm{e}^{\mathrm{i}\theta_{14}}|1110\rangle+\mathrm{e}^{\mathrm{i}\theta_{15}}|1111\rangle)\\&\otimes\eta^2(\mathrm{e}^{-\mathrm{i}\theta_0}\langle0000|-\mathrm{e}^{-\mathrm{i}\theta_1}\langle0001|-\mathrm{e}^{-\mathrm{i}\theta_2}\langle0010|+\mathrm{e}^{-\mathrm{i}\theta_3}\langle0011|\\&-\mathrm{e}^{-\mathrm{i}\theta_4}\langle0100|+\mathrm{e}^{-\mathrm{i}\theta_5}\langle0101|+\mathrm{e}^{-\mathrm{i}\theta_6}\langle0110|-\mathrm{e}^{-\mathrm{i}\theta_7}\langle0111|)\\&-\mathrm{e}^{-\mathrm{i}\theta_8}\langle1000|+\mathrm{e}^{-\mathrm{i}\theta_9}\langle1001|+\mathrm{e}^{-\mathrm{i}\theta_{10}}\langle1010|-\mathrm{e}^{-\mathrm{i}\theta_{11}}\langle1011|\\&+\mathrm{e}^{-\mathrm{i}\theta_{12}}\langle1100|-\mathrm{e}^{-\mathrm{i}\theta_{13}}\langle1101|-\mathrm{e}^{-\mathrm{i}\theta_{14}}\langle1110|+\mathrm{e}^{-\mathrm{i}\theta_{15}}\langle1111|)].\end{aligned}$$

(v) The final state under depolarizing noise

$$\begin{aligned}\rho_{\mathrm{outB_1B_2B_3B_4}} = \frac{1}{16(1-\omega)^4+16\,(\omega/3)^4}[&(1-\omega)^2(\mathrm{e}^{\mathrm{i}\theta_0}|0000\rangle+\mathrm{e}^{\mathrm{i}\theta_1}|0001\rangle+\mathrm{e}^{\mathrm{i}\theta_2}|0010\rangle\\&+\mathrm{e}^{\mathrm{i}\theta_3}|0011\rangle+\mathrm{e}^{\mathrm{i}\theta_4}|0100\rangle+\mathrm{e}^{\mathrm{i}\theta_5}|0101\rangle+\mathrm{e}^{\mathrm{i}\theta_6}|0110\rangle+\mathrm{e}^{\mathrm{i}\theta_7}|0111\rangle+\mathrm{e}^{\mathrm{i}\theta_8}|1000\rangle\\&+\mathrm{e}^{\mathrm{i}\theta_9}|1001\rangle+\mathrm{e}^{\mathrm{i}\theta_{10}}|1010\rangle+\mathrm{e}^{\mathrm{i}\theta_{11}}|1011\rangle+\mathrm{e}^{\mathrm{i}\theta_{12}}|1100\rangle+\mathrm{e}^{\mathrm{i}\theta_{13}}|1101\rangle\\&+\mathrm{e}^{\mathrm{i}\theta_{14}}|1110\rangle+\mathrm{e}^{\mathrm{i}\theta_{15}}|1111\rangle)\otimes(1-\omega)^2(\mathrm{e}^{-\mathrm{i}\theta_0}\langle0000|+\mathrm{e}^{-\mathrm{i}\theta_1}\langle0001|\\&+\mathrm{e}^{-\mathrm{i}\theta_2}\langle0010|+\mathrm{e}^{-\mathrm{i}\theta_3}\langle0011|+\mathrm{e}^{-\mathrm{i}\theta_4}\langle0100|+\mathrm{e}^{-\mathrm{i}\theta_5}\langle0101|+\mathrm{e}^{-\mathrm{i}\theta_6}\langle0110|\\&+\mathrm{e}^{-\mathrm{i}\theta_7}\langle0111|+\mathrm{e}^{-\mathrm{i}\theta_8}\langle1000|+\mathrm{e}^{-\mathrm{i}\theta_9}\langle1001|+\mathrm{e}^{-\mathrm{i}\theta_{10}}\langle1010|+\mathrm{e}^{-\mathrm{i}\theta_{11}}\langle1011|\\&+\mathrm{e}^{-\mathrm{i}\theta_{12}}\langle1100|+\mathrm{e}^{-\mathrm{i}\theta_{13}}\langle1101|+\mathrm{e}^{-\mathrm{i}\theta_{14}}\langle1110|+\mathrm{e}^{-\mathrm{i}\theta_{15}}\langle1111|)\\&+(\omega/3)^2\,(\mathrm{e}^{\mathrm{i}\theta_{15}}|0000\rangle+\mathrm{e}^{\mathrm{i}\theta_{14}}|0001\rangle+\mathrm{e}^{\mathrm{i}\theta_{13}}|0010\rangle+\mathrm{e}^{\mathrm{i}\theta_{12}}|0011\rangle\\&+\mathrm{e}^{\mathrm{i}\theta_{11}}|0100\rangle+\mathrm{e}^{\mathrm{i}\theta_{10}}|0101\rangle+\mathrm{e}^{\mathrm{i}\theta_9}|0110\rangle+\mathrm{e}^{\mathrm{i}\theta_8}|0111\rangle+\mathrm{e}^{\mathrm{i}\theta_7}|1000\rangle\\&+\mathrm{e}^{\mathrm{i}\theta_6}|1001\rangle+\mathrm{e}^{\mathrm{i}\theta_5}|1010\rangle+\mathrm{e}^{\mathrm{i}\theta_4}|1011\rangle+\mathrm{e}^{\mathrm{i}\theta_3}|1100\rangle+\mathrm{e}^{\mathrm{i}\theta_2}|1101\rangle\\&+\mathrm{e}^{\mathrm{i}\theta_1}|1110\rangle+\mathrm{e}^{\mathrm{i}\theta_0}|1111\rangle)\otimes(\omega/3)^2\,(\mathrm{e}^{-\mathrm{i}\theta_{15}}\langle0000|+\mathrm{e}^{-\mathrm{i}\theta_{14}}\langle0001|\\&+\mathrm{e}^{-\mathrm{i}\theta_{13}}\langle0010|+\mathrm{e}^{-\mathrm{i}\theta_{12}}\langle0011|+\mathrm{e}^{-\mathrm{i}\theta_{11}}\langle0100|+\mathrm{e}^{-\mathrm{i}\theta_{10}}\langle0101|+\mathrm{e}^{-\mathrm{i}\theta_9}\langle0110|\\&+\mathrm{e}^{-\mathrm{i}\theta_8}\langle0111|+\mathrm{e}^{-\mathrm{i}\theta_7}\langle1000|+\mathrm{e}^{-\mathrm{i}\theta_6}\langle1001|+\mathrm{e}^{-\mathrm{i}\theta_5}\langle1010|+\mathrm{e}^{-\mathrm{i}\theta_4}\langle1011|\\&+\mathrm{e}^{-\mathrm{i}\theta_3}\langle1100|+\mathrm{e}^{-\mathrm{i}\theta_2}\langle1101|+\mathrm{e}^{-\mathrm{i}\theta_1}\langle1110|+\mathrm{e}^{-\mathrm{i}\theta_0}\langle1111|)\\&+(\omega/3)^2\,\mathrm{i}(\mathrm{e}^{\mathrm{i}\theta_{15}}|0000\rangle-\mathrm{e}^{\mathrm{i}\theta_{14}}|0001\rangle-\mathrm{e}^{\mathrm{i}\theta_{13}}|0010\rangle+\mathrm{e}^{\mathrm{i}\theta_{12}}|0011\rangle\\&-\mathrm{e}^{\mathrm{i}\theta_{11}}|0100\rangle+\mathrm{e}^{\mathrm{i}\theta_{10}}|0101\rangle+\mathrm{e}^{\mathrm{i}\theta_9}|0110\rangle-\mathrm{e}^{\mathrm{i}\theta_8}|0111\rangle-\mathrm{e}^{\mathrm{i}\theta_7}|1000\rangle\\&+\mathrm{e}^{\mathrm{i}\theta_6}|1001\rangle+\mathrm{e}^{\mathrm{i}\theta_5}|1010\rangle-\mathrm{e}^{\mathrm{i}\theta_4}|1011\rangle+\mathrm{e}^{\mathrm{i}\theta_3}|1100\rangle-\mathrm{e}^{\mathrm{i}\theta_2}|1101\rangle\\&-\mathrm{e}^{\mathrm{i}\theta_1}|1110\rangle+\mathrm{e}^{\mathrm{i}\theta_0}|1111\rangle)\otimes(\omega/3)^2\,\mathrm{i}(\mathrm{e}^{-\mathrm{i}\theta_{15}}\langle0000|-\mathrm{e}^{-\mathrm{i}\theta_{14}}\langle0001|\end{aligned}$$

$$
\begin{aligned}
&-\mathrm{e}^{-\mathrm{i}\theta_{13}}\langle 0010|+\mathrm{e}^{-\mathrm{i}\theta_{12}}\langle 0011|-\mathrm{e}^{-\mathrm{i}\theta_{11}}\langle 0100|+\mathrm{e}^{-\mathrm{i}\theta_{10}}\langle 0101|+\mathrm{e}^{-\mathrm{i}\theta_{9}}\langle 0110|\\
&-\mathrm{e}^{-\mathrm{i}\theta_{8}}\langle 0111|-\mathrm{e}^{-\mathrm{i}\theta_{7}}\langle 1000|+\mathrm{e}^{-\mathrm{i}\theta_{6}}\langle 1001|+\mathrm{e}^{-\mathrm{i}\theta_{5}}\langle 1010|-\mathrm{e}^{-\mathrm{i}\theta_{4}}\langle 1011|\\
&+\mathrm{e}^{-\mathrm{i}\theta_{3}}\langle 1100|-\mathrm{e}^{-\mathrm{i}\theta_{2}}\langle 1101|-\mathrm{e}^{-\mathrm{i}\theta_{1}}\langle 1110|+\mathrm{e}^{-\mathrm{i}\theta_{0}}\langle 1111|)\\
&+(\omega/3)^2(\mathrm{e}^{\mathrm{i}\theta_0}|0000\rangle-\mathrm{e}^{\mathrm{i}\theta_1}|0001\rangle-\mathrm{e}^{\mathrm{i}\theta_2}|0010\rangle+\mathrm{e}^{\mathrm{i}\theta_3}|0011\rangle-\mathrm{e}^{\mathrm{i}\theta_4}|0100\rangle\\
&+\mathrm{e}^{\mathrm{i}\theta_5}|0101\rangle+\mathrm{e}^{\mathrm{i}\theta_6}|0110\rangle-\mathrm{e}^{\mathrm{i}\theta_7}|0111\rangle-\mathrm{e}^{\mathrm{i}\theta_8}|1000\rangle+\mathrm{e}^{\mathrm{i}\theta_9}|1001\rangle\\
&+\mathrm{e}^{\mathrm{i}\theta_{10}}|1010\rangle-\mathrm{e}^{\mathrm{i}\theta_{11}}|1011\rangle+\mathrm{e}^{\mathrm{i}\theta_{12}}|1100\rangle-\mathrm{e}^{\mathrm{i}\theta_{13}}|1101\rangle-\mathrm{e}^{\mathrm{i}\theta_{14}}|1110\rangle\\
&+\mathrm{e}^{\mathrm{i}\theta_{15}}|1111\rangle)\otimes(\omega/3)^2(\mathrm{e}^{-\mathrm{i}\theta_0}\langle 0000|-\mathrm{e}^{-\mathrm{i}\theta_1}\langle 0001|-\mathrm{e}^{-\mathrm{i}\theta_2}\langle 0010|+\mathrm{e}^{-\mathrm{i}\theta_3}\langle 011|\\
&-\mathrm{e}^{-\mathrm{i}\theta_4}\langle 0100|+\mathrm{e}^{-\mathrm{i}\theta_5}\langle 0101|+\mathrm{e}^{-\mathrm{i}\theta_6}\langle 0110|-\mathrm{e}^{-\mathrm{i}\theta_7}\langle 0111|\\
&-\mathrm{e}^{-\mathrm{i}\theta_8}\langle 1000|+\mathrm{e}^{-\mathrm{i}\theta_9}\langle 1001|+\mathrm{e}^{-\mathrm{i}\theta_{10}}\langle 0010|-\mathrm{e}^{-\mathrm{i}\theta_{11}}\langle 1011|\\
&+\mathrm{e}^{-\mathrm{i}\theta_{12}}\langle 1100|-\mathrm{e}^{-\mathrm{i}\theta_{13}}\langle 1101|-\mathrm{e}^{-\mathrm{i}\theta_{14}}\langle 1110|+\mathrm{e}^{-\mathrm{i}\theta_{15}}\langle 1111|)].
\end{aligned}
$$

(vi) The final state under bit-phase flip noise

$$
\begin{aligned}
\rho_{\mathrm{out}B_1B_2B_3B_4} = &\frac{1}{16(1-\gamma)^4+16\gamma^4}[(1-\gamma)^4(\mathrm{e}^{\mathrm{i}\theta_0}|0000\rangle+\mathrm{e}^{\mathrm{i}\theta_1}|0001\rangle\\
&+\mathrm{e}^{\mathrm{i}\theta_2}|0010\rangle+\mathrm{e}^{\mathrm{i}\theta_3}|0011\rangle+\mathrm{e}^{\mathrm{i}\theta_4}|0100\rangle+\mathrm{e}^{\mathrm{i}\theta_5}|0101\rangle\\
&+\mathrm{e}^{\mathrm{i}\theta_6}|0110\rangle+\mathrm{e}^{\mathrm{i}\theta_7}|0111\rangle+\mathrm{e}^{\mathrm{i}\theta_8}|1000\rangle+\mathrm{e}^{\mathrm{i}\theta_9}|1001\rangle+\mathrm{e}^{\mathrm{i}\theta_{10}}|1010\rangle\\
&+\mathrm{e}^{\mathrm{i}\theta_{11}}|1011\rangle+\mathrm{e}^{\mathrm{i}\theta_{12}}|1100\rangle+\mathrm{e}^{\mathrm{i}\theta_{13}}|1101\rangle+\mathrm{e}^{\mathrm{i}\theta_{14}}|1110\rangle+\mathrm{e}^{\mathrm{i}\theta_{15}}|1111\rangle)\\
&\otimes(\mathrm{e}^{-\mathrm{i}\theta_0}\langle 0000|+\mathrm{e}^{-\mathrm{i}\theta_1}\langle 0001|+\mathrm{e}^{-\mathrm{i}\theta_2}\langle 0010|+\mathrm{e}^{-\mathrm{i}\theta_3}\langle 0011|+\mathrm{e}^{-\mathrm{i}\theta_4}\langle 0100|\\
&+\mathrm{e}^{-\mathrm{i}\theta_5}\langle 0101|+\mathrm{e}^{-\mathrm{i}\theta_6}\langle 0110|+\mathrm{e}^{-\mathrm{i}\theta_7}\langle 0111|+\mathrm{e}^{-\mathrm{i}\theta_8}\langle 1000|+\mathrm{e}^{-\mathrm{i}\theta_9}\langle 1001|\\
&+\mathrm{e}^{-\mathrm{i}\theta_{10}}\langle 1010|+\mathrm{e}^{-\mathrm{i}\theta_{11}}\langle 1011|+\mathrm{e}^{-\mathrm{i}\theta_{12}}\langle 1100|+\mathrm{e}^{-\mathrm{i}\theta_{13}}\langle 1101|+\mathrm{e}^{-\mathrm{i}\theta_{14}}\langle 1110|\\
&+\mathrm{e}^{-\mathrm{i}\theta_{15}}\langle 1111|)+\gamma^4(\mathrm{e}^{\mathrm{i}\theta_{15}}|0000\rangle-\mathrm{e}^{\mathrm{i}\theta_{14}}|0001\rangle-\mathrm{e}^{\mathrm{i}\theta_{13}}|0010\rangle\\
&+\mathrm{e}^{\mathrm{i}\theta_{12}}|0011\rangle-\mathrm{e}^{\mathrm{i}\theta_{11}}|0100\rangle+\mathrm{e}^{\mathrm{i}\theta_{10}}|0101\rangle+\mathrm{e}^{\mathrm{i}\theta_{9}}|0110\rangle\\
&-\mathrm{e}^{\mathrm{i}\theta_{8}}|0111\rangle-\mathrm{e}^{\mathrm{i}\theta_{7}}|1000\rangle+\mathrm{e}^{\mathrm{i}\theta_{6}}|1001\rangle+\mathrm{e}^{\mathrm{i}\theta_{5}}|1010\rangle\\
&-\mathrm{e}^{\mathrm{i}\theta_{4}}|1011\rangle+\mathrm{e}^{\mathrm{i}\theta_{3}}|1100\rangle-\mathrm{e}^{\mathrm{i}\theta_{2}}|1101\rangle-\mathrm{e}^{\mathrm{i}\theta_{1}}|1110\rangle+\mathrm{e}^{\mathrm{i}\theta_{0}}|1111\rangle)\\
&\otimes(\mathrm{e}^{-\mathrm{i}\theta_{15}}\langle 0000|-\mathrm{e}^{-\mathrm{i}\theta_{14}}\langle 0001|-\mathrm{e}^{-\mathrm{i}\theta_{13}}\langle 0010|+\mathrm{e}^{-\mathrm{i}\theta_{12}}\langle 0011|\\
&-\mathrm{e}^{-\mathrm{i}\theta_{11}}\langle 0100|+\mathrm{e}^{-\mathrm{i}\theta_{10}}\langle 0101|+\mathrm{e}^{-\mathrm{i}\theta_{9}}\langle 0110|-\mathrm{e}^{-\mathrm{i}\theta_{8}}\langle 0111|-\mathrm{e}^{-\mathrm{i}\theta_{7}}\langle 1000|\\
&+\mathrm{e}^{-\mathrm{i}\theta_{6}}\langle 1001|+\mathrm{e}^{-\mathrm{i}\theta_{5}}\langle 1010|-\mathrm{e}^{-\mathrm{i}\theta_{4}}\langle 1011|+\mathrm{e}^{-\mathrm{i}\theta_{3}}\langle 1100|-\mathrm{e}^{-\mathrm{i}\theta_{2}}\langle 1101|\\
&-\mathrm{e}^{-\mathrm{i}\theta_{1}}\langle 1110|+\mathrm{e}^{-\mathrm{i}\theta_{0}}\langle 1111|)].
\end{aligned}
$$

Finally, we can get the fidelities of prepared four-qubit equatorial states in a noisy environment as shown in Eqs. (35)–(40).

Acknowledgment

Project supported by the Fundamental Research Program of Shanxi Province (Grant No. 202203021211260).

References

[1] Bennett C H, Brassard G, Crépeau C, *et al.* 1993 *Phys. Rev. Lett.* **70** 1895
[2] Bouwmeester D, Pan J W, Mattle K, *et al.* 1997 *Nature* **390** 575
[3] Gottesman D 2000 *Phys. Rev. A* **61** 042311
[4] Singh S K and Srikanth R 2005 *Phys. Rev. A* **71** 012328
[5] Long G L and Liu X S 2002 *Phys. Rev. A* **65** 032302
[6] Deng F G and Long G L 2004 *Phys. Rev. A* **69** 052319
[7] Zhang W, Ding D S, Sheng Y B, *et al.* 2017 *Phys. Rev. Lett.* **118** 220501
[8] Zhou L, Sheng Y B and Long G L 2020 *Sci. Bull.* **65** 12
[9] Bennett C H, DiVincenzo D P, Shor P W, *et al.* 2001 *Phys. Rev. Lett.* **87** 077902
[10] Pati A K 2000 *Phys. Rev. A* **63** 014302
[11] Berry D W and Sanders B C 2003 *Phys. Rev. Lett.* **90** 057901
[12] Li J F, Liu J M, Feng X L and Oh C H 2016 *Quantum Inf. Process.* **15** 2155
[13] Nguyen B A, Cao T B, Nung V D and Kim J 2011 *Adv. Nat. Sci.: Nanosci. Nanotechnol.* **2** 035009
[14] Nguyen B A 2010 *Opt. Commun.* **283** 4113
[15] Liu H H, Cheng L Y, Shao X Q, *et al.* 2011 *Int. J. Theor. Phys.* **50** 3023
[16] Zhang C Y, Bai M Q and Zhou S Q 2018 *Quantum Inf. Process.* **17** 146
[17] Gong R and Jiang M 2022 *J. Opt. Soc. Am. B* **39** 3066

[18] Gong R, Wei Y, Xue S and Jiang M 2022 *Quantum Inf. Process.* **21** 341
[19] Huang L and Zhao H X 2017 *Int. J. Theor. Phys.* **56** 678
[20] Chen X B, Ma S Y, Su Y, *et al.* 2012 *Quantum Inf. Process.* **11** 1653
[21] Kiktenko E O, Popov A A and Fedorov A K 2016 *Phys. Rev. A* **93** 62305
[22] Zhang D, Zha X W, Duan Y J and Wei Z H 2016 *Int. J. Theor. Phys.* **55** 440
[23] Zhang D, Zha X W, Duan Y J and Yang Y Q 2016 *Quantum Inf. Process.* **15** 2169
[24] Chen X B, Sun Y R, Xu G and Jia H Y 2017 *Quantum Inf. Process.* **16** 244
[25] Gu J R and Liu J M 2022 *Commun. Theor. Phys.* **74** 075101
[26] Paris M G A, Cola M and Bonifacio R 2003 *J. Opt. B* **5** S360
[27] Kurucz Z, Adam P, Kis Z and Janszky J 2005 *Phys. Rev. A* **72** 052315
[28] Rådmark M , Wieśniak M, Żukowski M and Bourennane M 2013 *Phys. Rev. A* **88** 032304
[29] Xiang G Y, Li J, Yu B and Guo G C 2015 *Phys. Rev. A* **72** 012315
[30] Liu W T, Wu W and Ou B Q, *et al.* 2007 *Phys. Rev. A* **76** 022308
[31] Barreiro J T, Wei T C and Kwiat P G 2010 *Phys. Rev. Lett.* **105** 030407
[32] Wei D X, Luo J and Yang X D 2004 *Chin. Phys.* **13** 817
[33] Nielsen M A and Chuang I L 2000 *Quantum Computation and Quantum Information* (Cambridge University Press)
[34] Guan X W, Chen X B and Wang L C 2014 *Int. J. Theor. Phys.* **53** 2236
[35] Li J F, Liu J M and Xu X Y 2015 *Quantum Inf. Process.* **14** 3465
[36] Wang M M and Qu Z G 2016 *Quantum Inf. Process.* **15** 4805
[37] Wang M M, Qu Z G and Wang W 2017 *Quantum Inf. Process.* **16** 140
[38] Li Y H, Wang Z S and Zhou H Q 2019 *Int. J. Theor. Phys.* **58** 1172
[39] Zhang P, Ma S and Gong L 2019 *Int. J. Theor. Phys.* **58** 2795
[40] Qian Y, Xue S and Jiang M 2020 *Phys. Lett. A* **384** 126204
[41] Dash T, Sk R and Panigrahi P K 2020 *Opt. Commun.* **464** 125518
[42] Xu Z, Wei Y, Jiang C and Jiang M 2022 *Chin. Phys. B* **31** 040304
[43] Huelga S F, Vaccaro J A, Cheflfles A and Plenio M B 2001 *Phys. Rev. A* **63** 042303
[44] Wu L A and Lidar D A 2002 *Phys. Rev. A* **67** 050303
[45] Buscemi F, DAriano G M and Macchiavello C 2005 *Phys. Rev. A* **71** 042327
[46] Rezakhani A T, Siadatnejad S and Ghaderi A H 2005 *Phys. Lett. A* **336** 278
[47] Kang P, Dai H Y, Wei J H and Zhang M 2016 *Phys. Rev. A* **94** 042304
[48] Chen Q Q, Xia Y and Song J 2011 *Opt. Commun.* **284** 5031
[49] Choudhury B S and Dhara A 2015 *Quantum Inf. Process.* **14** 373
[50] Li X H and Ghose S 2015 *Quantum Inf. Process.* **14** 4585
[51] Adepoju A G, Falaye B J and Sun G H 2017 *Phys. Lett. A* **381** 581
[52] Sun Y R, Xu G and Chen X B 2018 *IEEE Access* **7** 2811
[53] Wei J H, Shi L, Zhu Y, *et al.* 2018 *Quantum Inf. Process.* **17** 70
[54] Sun Y R, Chen X B, Xu G, *et al.* 2019 *Sci. Rep.* **9** 2081
[55] Sun Y R, Chen Y L Ahmad H and Wei Z H 2019 *Computers, Materials and Continua* **59** 215
[56] Zha X W, Wang M R and Jiang R X 2020 *Chin. Phys. B* **29** 040304
[57] Wang M R, Xiang Z and Ren P 2022 *Mod. Phys. Lett. B* **36** 2250078
[58] Bellomo B, Lo Franco R and Compagno G 2008 *Phys. Rev. A* **77** 032342
[59] Peng J Y and Xiang Y 2021 *Opt. Commun.* **499** 127285